



Analytical applications for pore-forming proteins[☆]



John J. Kasianowicz^{a,*}, Arvind K. Balijepalli^a, Jessica Ettetdgui^a, Jacob H. Forstater^a, Haiyan Wang^a, Huisheng Zhang^b, Joseph W.F. Robertson^a

^a NIST, Physical Measurement Laboratory, Gaithersburg, MD 20899, United States

^b Guangdong Key Laboratory for Biomedical Measurements and Ultrasound Imaging, Dept. of Biomedical Engineering, School of Medicine, Shenzhen University, Shenzhen 518060, China

ARTICLE INFO

Article history:

Received 6 July 2015

Received in revised form 28 August 2015

Accepted 25 September 2015

Available online 22 October 2015

Keywords:

Nanopore

Hemolysin

Pore forming toxin

DNA sequencing

Force spectroscopy

Temperature-jump spectroscopy

ABSTRACT

Proteinaceous nanometer-scale pores are ubiquitous in biology. The canonical ionic channels (e.g., those that transport Na⁺, K⁺, Ca²⁺, and Cl⁻ across cell membranes) play key roles in many cellular processes, including nerve and muscle activity. Another class of channels includes bacterial pore-forming toxins, which disrupt cell function, and can lead to cell death. We describe here the recent development of these toxins for a wide range of biological sensing applications. This article is part of a Special Issue entitled: Pore-Forming Toxins edited by Mauro Dalla Serra and Franco Gambale.

Published by Elsevier B.V.

1. Introduction

The study of giant squid axons during the late 1930s through the early 1950s led to the conclusion that there were separate pathways for Na⁺ and K⁺ transport in nerve fibers [1–6]. A theoretical analysis by Parsegian showed that a water-filled pore provides the lowest energy barrier for ion transport through cell membranes [7], and these portals were only recently shown to be formed by proteins [6,8–10]. Transmembrane protein channels are also the molecular basis of other cellular functions, including water transport across cells [11–13], cell–cell communication [14], and muscle activity [15]. Their malfunction can cause debilitating and deadly diseases [12,16,17], which range from cardiac dysfunction [18] to cystic fibrosis [19]. Channels are nanometer-scale in length and breadth, and their narrow confines, in part, confer ion selectivity to them [20] which is essential to their proper function.

Another class of channels is the family of pore-forming toxins, which are secreted by bacteria [21–23]. Examples of these include *Staphylococcus aureus* alpha-hemolysin (α HL) [24,25], *Mycobacterium smegmatis* MspA [26], *Escherichia coli* OmpF [27], and *Bacillus brevis* gramicidin [28]. The putative structures for these porins are illustrated in Fig. 1. While understanding the mechanisms of action for bacterial pore-forming toxins is vitally important, we discuss here only their

development for use in the detection, identification, quantification, and physical characterization of single molecules [29–32].

We will confine most of the discussion below to the channel formed by α HL, because its properties have proven useful for much of the applied nanopore-based sensor research that has been done to date. Briefly, α HL is a pore-forming leukotoxin [25,33] that spontaneously binds to membranes and forms a pore from seven identical subunits [34]. The crystal structure of the channel shows that it contains a conical vestibule, located outside the membrane and a β -barrel segment that spans the membrane [35]. These two components are separated by a narrow constriction, and the nature of the interaction of molecules with the pore can depend on which side of the pore they enter [36,37].

2. Development of nanopores as single molecule sensors

While it might seem unconventional, the use of single channels for sensing applications has a precedent in biology. For example, receptor channels, located at neural synapses, change their conducting state as a function of neurotransmitter concentration. In the late 1980s, several experimental findings made it possible to consider whether these nanometer-scale entities might prove useful for detecting and characterizing individual molecules electronically with high impedance amplifiers (Fig. 2).

2.1. Impediments to channel-based sensor development

The method seems simple at first glance. The entry of an analyte into the pore will alter the ionic current that otherwise flows freely by either

[☆] This article is part of a Special Issue entitled: Pore-Forming Toxins edited by Mauro Dalla Serra and Franco Gambale.

* Corresponding author.

E-mail address: john.kasianowicz@nist.gov (J.J. Kasianowicz).

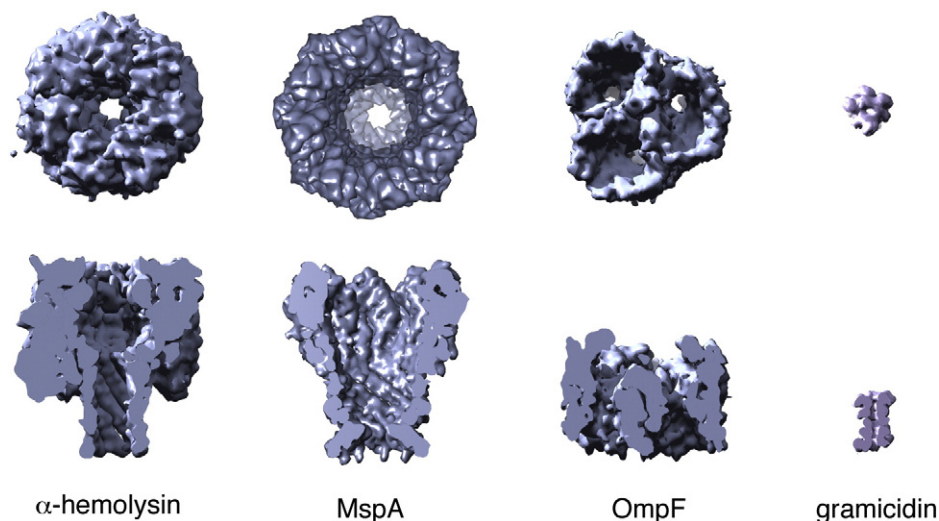


Fig. 1. Putative structures of the pore-forming toxins *Staphylococcus aureus* alpha-hemolysin (α HL) PDB: 7AHL [35], MspA PDB: 1UUN [212], OmpF PDB: 2OMF [213], *Bacillus brevis* gramicidin PDB: 1GRM [214].

altering the electrostatic potential profile across the pore [38,39] (Fig. 3, left), or via volume exclusion and adsorption of mobile ions [40, 41](Fig. 3, center). In addition, an analyte could inhibit pore formation or decrease the pore conductance, and the target analyte concentration would be inferred from the loss of ionic current [42,43] (Fig. 3, right). For the first two schemes, several issues had to be resolved to enable single molecule sensing with nanopores.

First, channels tend to gate spontaneously (i.e., switch between different conducting states), which would obviously confound their

use as sensors. Indeed, Gianfranco Menestrina demonstrated that the *S. aureus* α HL channel gates from the fully open to lesser conductance states with relatively slow kinetics (tens of seconds) [25] compared to those for mammalian Na^+ and K^+ channels (milliseconds). Importantly, he also showed that the channel gates more quickly in the presence of divalent and trivalent cations. Serendipitously, we found that other factors could alter the α HL channel gating kinetics, and due to Menestrina's work, we were able to put the results into a useful context. Fig. 4 (left) illustrates that the conductance equivalent

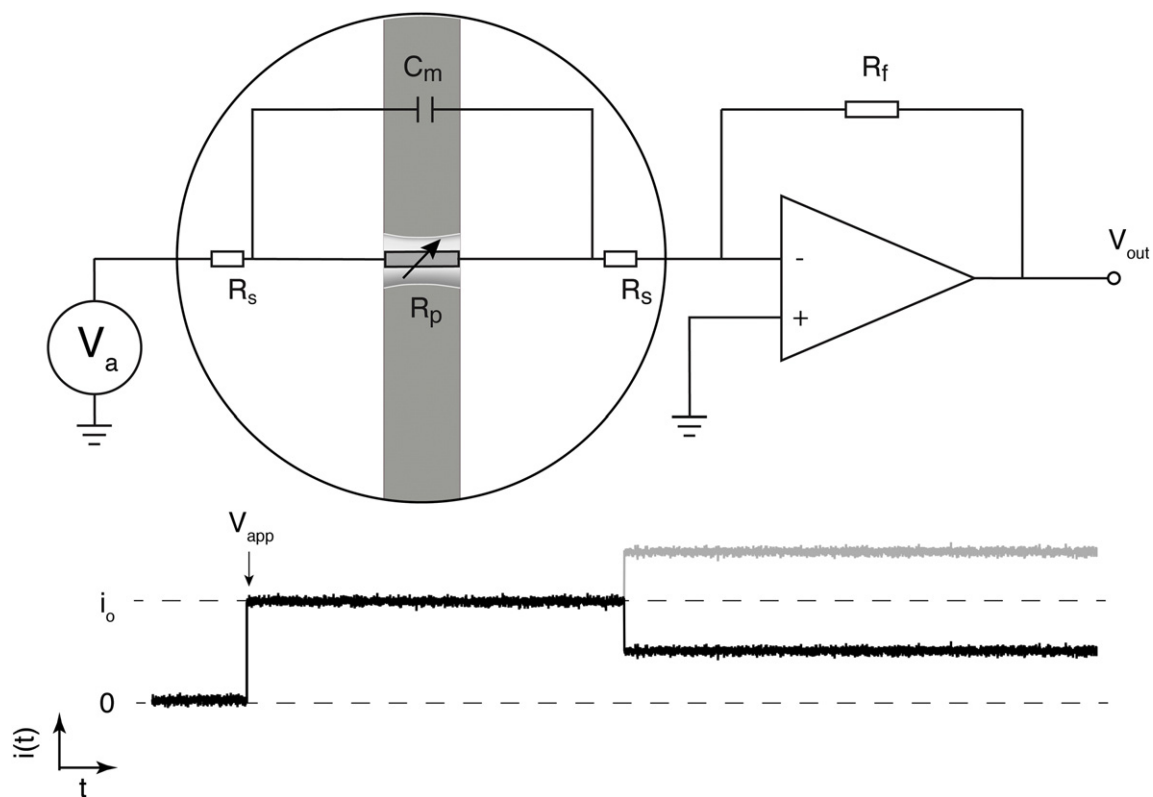


Fig. 2. Single nanopore current measurements. (Top) A single nanopore is embedded in a planar lipid bilayer membrane bathed on both sides by an aqueous electrolyte solution. The membrane is represented by a capacitor (C_m), the solutions as resistors (R_s) and the pore as a variable resistor (R_p , which is modulated by analytes). The pore current is measured by applying an electrostatic potential (V_a) via two Ag–AgCl electrodes (not shown), and a low-noise, high-impedance amplifier. (Bottom) The fully open pore current, i_0 , can increase or decrease when an analyte enters the pore.

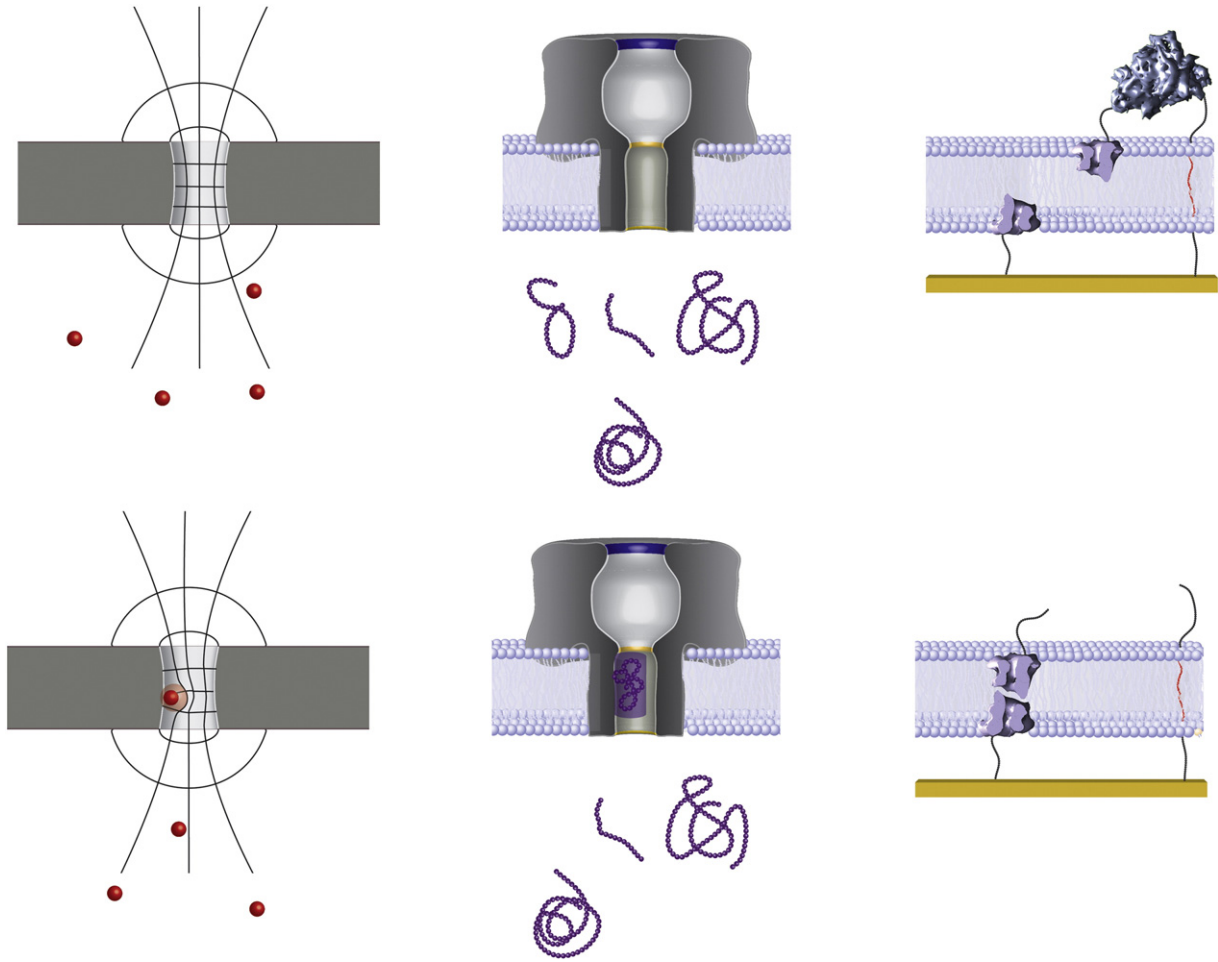


Fig. 3. Several mechanisms for nanopore-based detection of analytes. (Left) The analyte causes a change in the electric field inside or near the pore [38,39]. (Center) The analyte reduces the ionic current flow through the pore due to volume exclusion and the binding of mobile ions to the analyte [40,41,44,45]. (Right) The binding of an analyte to both a fixed receptor and a site on the upper half of a channel formed by dimers (i.e., gramicidin) reduces pore formation [42].

of ~100 α HL channels gate more rapidly as the applied potential is increased. However, at a fixed applied potential, as the pH is increased, the gating kinetics were slowed (Fig. 4, center). Increasing the monovalent 1:1 electrolyte concentration had the same effect (Fig. 4, right). These results provided the means to keep the α HL channel open indefinitely and initially demonstrate its usefulness in sensing applications [38,39,44–46]. For example, the α HL pore was subsequently used to quantitate the concentration hydronium and deuterium ions and discriminate between the two isotopes [38,39].

Second, even though the α HL channel could remain open for minutes or hours, another kinetic issue remained. Assuming the pore spans a 4 nm thick membrane, for diffusion-controlled trajectories [47], the time that a single molecule would spend inside the pore (~50 ns) would be far too short to detect with a high impedance amplifier. Specifically, the RC time constant of the system is ~1 μ s, and the number of ions that would flow past an analyte in the pore in that time (~50 ions/50 ns) is statistically too small to extract any useful information about a molecule [29]. As we discuss below, this issue was

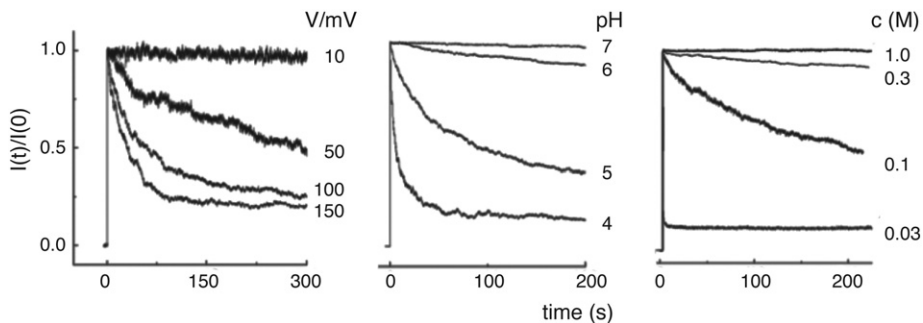


Fig. 4. Controlling nanopore gating. The rate at which α HL channels close decreases with decreasing applied potential (left), increasing pH (center), and increasing monovalent electrolyte concentration (right) [39] (Kasianowicz, J.J. unpublished). The membranes contained ~100 channel equivalents of α HL.

resolved with another serendipitous experimental finding stimulated by the work of Oleg Krasilnikov.

2.2. Probing pore geometry with non-electrolyte polymers

The use of non-electrolyte polymers to probe the volume and dimensions of ion-channels is largely attributable to the pioneering work of Zimmerberg and Parsegian [48,49] in the late 1980s and Krasilnikov and colleagues reported in the early 1990s [50]. Zimmerberg and Parsegian demonstrated that pore-impermeant non-electrolyte polymers could be used to estimate the volume change associated with gating of the mitochondrial voltage-dependent anion channel (VDAC). Here, the polymer draws water out of the pore via osmotic pressure (the work done by that pressure causes the pore volume to decrease). This technique has been adopted in structural biology, by using the osmolytes to inhibit or control the conformation of porins for high resolution structural techniques such as electron paramagnetic resonance [51].

Krasilnikov and colleagues developed another polymer-based method to probe ion channel geometry [50,52–55]. It was known that the addition of non-electrolyte polymer poly(ethylene glycol) (PEG) to an aqueous electrolyte solution lowered the latter's bulk conductivity. Krasilnikov reasoned that only those polymers that were sufficiently small to enter the pore would reduce the channel ionic conductance. This method has been used to “size” channels formed by *S. aureus* α HL [50,54–58], *Bacillus anthracis* protective antigen 63 [59–61], chrysospermin [62], nonpeptidic fungal toxin [63], the α - and β -subunits of cholera enterotoxin [64], syringomycin E [65], *Vibrio cholera* cytolysin [66], *Pasteurella multocida* dermonecrotic toxin [67], colicin Ia [68], VDAC from mitochondria [69], and the malaria parasite's nutrient channel [70].

A biological nanopore can be approximated as a resistor formed by an electrolyte-filled right circular cylinder of radius, r , and length, l , filled with an electrolyte with bulk conductivity, σ [5]. Under these idealized conditions, the radius of the nanopore can be estimated by measuring the nanopore resistance: $R = l / (\pi r^2 \sigma)$. This simple approach ignores several important details. Biological nanopores are not perfect cylinders; rather, they frequently contain one or more constrictions of varying dimensions and often exhibit significant axial asymmetry. Also, because of the nanopore's restrictive volume and fixed charged residues, the channel conductance may not scale directly with the bulk solution conductivity. Furthermore, within the nanopore water is highly structured further changing the diffusivity of electrolytes across the channel and affecting the conductance. [41,71–73] While these techniques demonstrate that polymers can partially occlude the pore, they do not provide information about the location of the limiting constriction.

More detailed information about the structure, size, and location of varying features can be inferred by examining the partitioning of non-electrolyte polymers added to each side of the pore. If the pore is geometrically asymmetric, the polymer accessibility from each side could differ and the conductance of the nanopore can be decomposed into two parts, one representing the contribution of the non-electrolyte polymer filling the pore and the other due to the contribution of the polymer-free solution. Moreover, smaller polymers should penetrate deeper into the pore, which can provide spatially-resolved information by defining a dimensionless filling factor, which describes the relative contributions of these two components:

$$F = \frac{\left(\frac{g_0 - g_i}{g_i} \right)}{\left(\frac{\chi_0 - \chi_i}{\chi_i} \right)}$$

where g_0 and g_i are the conductance of the polymer-filled and polymer free nanopore, respectively, and χ_0 and χ_i are the conductivities of the polymer-filled and polymer-free electrolyte solutions, respectively [36,

68,74]. Using this approach, Krasilnikov and colleagues were able to obtain surprisingly detailed measurements of the α HL channel geometry [36] that were nearly identical to the x-ray crystallographic data [35]. The polymer approach overestimated the actual size of the nanopore, in part, because the commercial PEG used in those studies were polydisperse.

2.3. Turning the tide: Probing polymers with nanopores

The results in Fig. 5 illustrate Krasilnikov's method for using polymers to probe pores, and how the opposite could be true. As expected, the current through a fully open single α HL channel is quiescent in the absence of PEG, and PEGs 200 and 2000, but not 8000 MW, apparently enter the pore and reduce the mean current (Fig. 5A). However, Kasianowicz and colleagues noticed that the current noise in the presence of PEG2000 was anomalously high (Fig. 5A) [44]. Fig. 5B shows that the mean excess current noise is far greater than one would expect if the polymer diffuses through the pore at a normal rate, which suggested the polymer interacts with the pore and thereby resides in the pore long enough to be detected [44] and later characterized at high resolution [40,41]. The polymer partitioning curve in Fig. 5C shows that the dependence of mean current on the mean PEG molecular weight does not follow a simple hard sphere interaction model, which further suggested a significant polymer–pore interaction [41,44,73]. These results made possible the use of pores to detect and characterize individual polymers.

Another method to use nanopores as sensors was developed using crown ethers (essentially a cyclized PEG) [75]. Here, Bezrukov, Krasilnikov and colleagues demonstrated a strong dependence on the residence time of the 18-crown-6, a well-known K^+ chelator, on the K^+ concentration. The results demonstrate that reversible reactions between the electrolyte and polymer of interest can be used to alter the residence time of the polymer in the nanopore. The initial demonstration of PEG's relatively long-lived residence time in the pore was done with relatively high monovalent electrolyte concentration (1 M NaCl) [44] compared to the earlier pore-sizing work (100 mM KCl) [50]. A further increase in the ionic strength (i.e., 4 M KCl), individual polymer–pore interactions can easily be observed unimodal resistive pulses with well-defined blockades that scale to first order with the polymer size [44,55], but in that study, the manufacturer's estimated molecular mass averages of the polydisperse polymers were used to deduce what limits PEG partitioning into the pore.

However, far more information can be gleaned by a more critical analysis of the individual polymer-induced current blockades (Fig. 6, bottom left). By characterizing each event and constructing a histogram of the mean ionic current level (with respect to that of the fully open and unoccupied pore), a polymer size spectrogram can be generated [40] (Fig. 6, top right). Using a highly purified monodisperse PEG, and comparing the results to those of the same polymer samples analyzed via MALDI-TOF mass spectrometry, each peak in a polydisperse PEG sample was shown to correspond to different sized polymers resolved to much better than the monomer mass limit (44 g/mol) [40]. This technique was coined “single molecule mass spectrometry” (SMMS) due to the similarity of the data's appearance to traditional high-vacuum mass spectrometry results, despite the fact that its physical origins more closely resemble solution-based separation techniques such as HPLC or capillary electrophoresis. The residence time distributions for the differently sized PEG molecules are fit well by single exponentials (Fig. 6, bottom right), which suggested the interaction between the polymers and the pore can be treated as a simple reversible first order chemical reaction [40,41]. The development of new membrane systems, such as high-bandwidth quartz capillary supports [76,77], robust polymerized membrane systems [78–80], high throughput microdrop arrays [81] and microfabricated membrane arrays [82–84] is enabling nanopore sensing to eventually leave the specialist's lab and promises to make

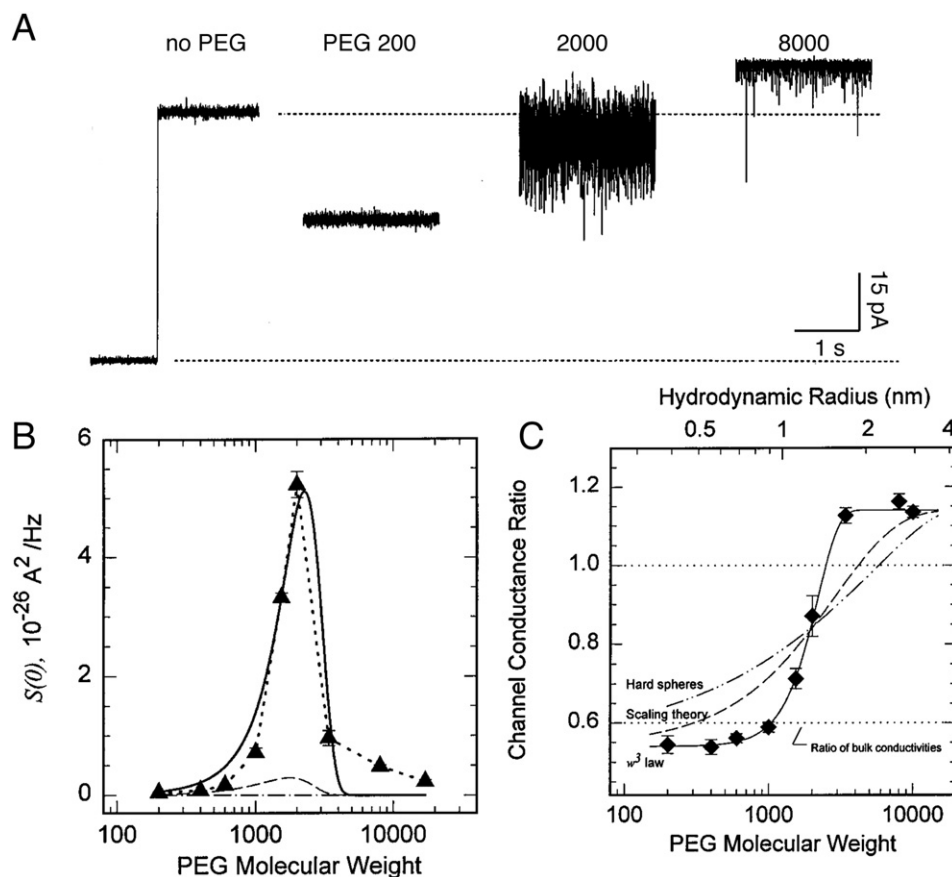


Fig. 5. Using polymers to physically characterize nanopores led to the use of pores for detecting and characterizing polymers. (A) Polymers of poly(ethylene glycol) that are sufficiently small enter the α HL pore (PEG 200 and 2000 mean molecular weight) and reduce the mean ionic current (filtered with a 1 kHz low pass filter). (B) The marked excess current noise caused by PEG 2000 suggested that the polymer interacts strongly with the pore. (C) The effect of different size PEGs on the mean current was not described by a simple hard sphere model, and further suggested that the polymer and the pore interact with each other [44,215].

nanopore sensing a routine tool for clinical and other analytical laboratories.

Taking advantage of the interactions of polymers with ions and the nanopore will ultimately enable SMMS as a viable analytical spectroscopic method. However, pores and polymers often do not have any inherent affinity for each other. In the limit of weak analyte–nanopore interactions, it is often necessary to develop sensors that rely on the interaction of the polymer with a second affinity reagent to extend the interaction long enough for the resistive pulse to resolve itself [85]. One successful strategy is to use a well-defined molecular adapter such as beta-cyclodextrin to restrict flow through the pore and modify the chemical interaction sites within the pore [86–88]. In a similar vein, it is possible to trap small gold clusters in the *cis*-side vestibule of α HL [89,90]. Because these clusters are too large to cross the internal constriction of α HL, the cluster's residence time can extend for arbitrarily long times. By carefully choosing the protective chemistry of the cluster, such as using negatively-charged glutathione staples, it is possible to use the metallic cluster to enhance the resolution of adjacent peaks in an SMMS experiment [91].

2.4. Theoretical understanding provides direction

For a homopolymeric system, such as a mixture of PEGs over a wide size range, SMMS provides a fully quantitative complimentary measurement to traditional mass spectrometry for simple routine chemical analysis [40]. However it also provides a rich experiment for the theoretical study of more general nanopore–polymer physics, which is important for the rational development of nanopore-based sensors.

As shown in Fig. 6, the interaction of analytes with a nanopore primarily gives rise to two observable quantities: the mean residence time of the molecule in the pore, and the change in channel conductance [40,45]. Not surprisingly, each individual interaction contains a time average of the molecule dynamics that are often too fast to be measured experimentally. Nevertheless, in many cases these interactions can be quantified through theoretical modeling of the underlying physical processes that govern pore–molecule interactions. Recent theoretical and computational work focused on such efforts [41,71,73, 92–94]. Here, we briefly describe the physical processes that give rise to the residence time distributions and blockade depths.

2.5. Mean residence times

Fig. 6 shows that the mean residence time of PEG in the pore is determined by its size, charge and shape. The latter two properties are codependent and strongly influence the observed distribution. For molecules with a fixed charge (i.e. DNA, polypeptides, etc.) transport across the pore occurs via diffusion with drift. For an ensemble of molecules, it is straightforward to model this process using the Fokker-Planck equation [41,73,95–99]. In the low Reynolds number regime, this equation further reduces to the Smoluchowski equation [94,100]. With appropriate boundary conditions, the solution of the residence times should follow a normal distribution, as verified experimentally [94]. In contrast, the residence times of molecules with mobile adsorbed charges can be strongly influenced by the kinetics of ion–analyte interactions [41]. PEG forms crown-ether-like complexes by coordinating cations in the gas phase (and in solution) via its oxygens [73,101]. Furthermore, the interactions between the two species follow first order kinetics, and

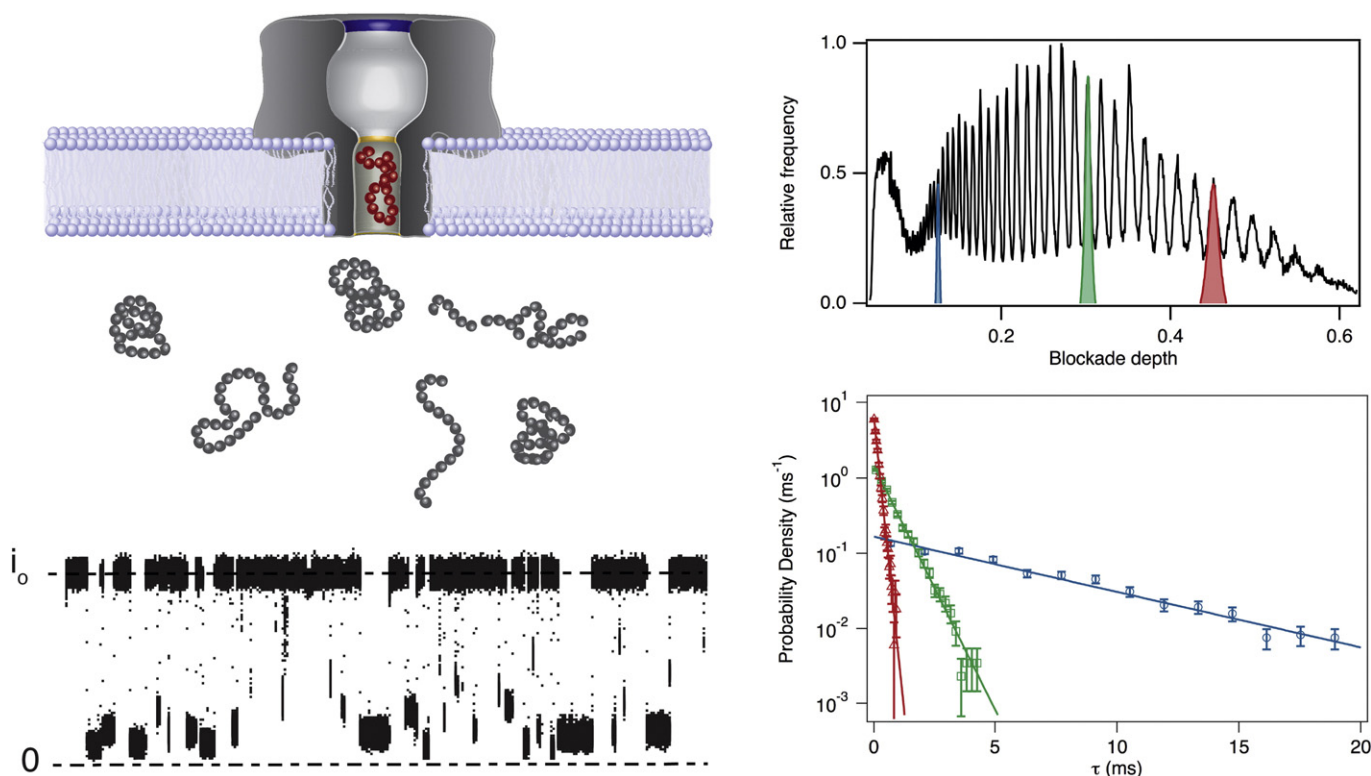


Fig. 6. High-resolution separation of individual polymers with a nanopore. (*Top left*) Individual polymers enter the pore stochastically. (*Bottom left*) Each polymer transiently reduces the pore's ionic current. (*Top right*) A histogram of the current blockade depth for thousands of events allows the polymers to be separated based on their size [40,41] and the charge adsorbed to them [41]. (*Bottom right*) The residence time distribution of many events provides a second estimator for polymer size [40,41]. Larger polymers block the current more than do smaller ones, and spend more time in the pore, on average.

the resulting distribution of residence times in the channel should therefore follow a single exponential [41]. They do (Fig. 6, *bottom right*) [40,41,102]. By combining the effects of chain entropy and cation-PEG binding kinetics, Reiner et al. modeled the mean residence time of PEG in the α HL nanopore as a free energy barrier profile with barriers [31,41]. The results show excellent agreement over a wide range of polymer sizes and for different values of the applied potential. The results were further improved using molecular dynamics (MD) simulations of PEG in the pore [73]. Parameters such as the mean number of bound cations, coordination number and geometry of the confined chain were used to extend the size range of the measurement, and improve the agreement with theory.

2.6. Channel conductance

The decrease in the channel conductance caused by the entry of a single molecule into the pore is primarily caused by volume exclusion. This simple statement, while non-controversial, fails to describe many of the interesting details observed for a simple homopolymer system such as PEG, or even the different bases of DNA. Simplifying approximations for the blockade of a micron-scale pore were made by DeBlois and Bean as early as the 1970s [103]. Specifically, for this simple model, two regimes emerge that where either the volume of the pore or the cross-sectional area is significantly filled. This approach works well for a majority of larger nanopore systems, such as those fabricated to look more like a Coulter counter [104–108]. However, these approaches fail when applied to systems such as PEGs and α HL, because of the intricacies arising from polymer dynamics and chemical interactions in the extremely confined environment of the pore cavity [109]. In an early attempt to describe the PEG system, Bezukov used a concept of “microviscosity” to characterize the drag induced on a single particle

in a confined environment [55,110]. Although not explicitly stated, this *ansatz* was actually based on Mooney's extension of Einstein's theory for the viscosity of spherical particles in solution [111]. The microviscosity treatment roughly fits the conductance dependence on the PEG molecular weight (i.e., an exponentially decreasing conductance with increasing polymer size). However the relatively few data points used in the study [55], and the lack of monomer-level resolution precluded an accurate theoretical treatment. Using the monomer-resolved spectrogram [40], Reiner and colleagues modeled the blockade depth by describing the polymer system in terms of both volume exclusion and ion polymer interactions [41]. By incorporating both interaction types, a detailed thermodynamic model was used to fit both conductance fluctuations and residence times, which was not addressed by the earlier simple model.

The dissociation constants for PEG binding to monovalent cations varies with the cation type [112], but they are generally ≈ 1 M [40,44, 50,55,112], i.e., the binding is very weak. Let's assume the reaction is first order and the dissociation constant is $K_d = k_{off} / k_{on}$, where k_{off} and k_{on} are the rate constants for the dissociation and association of cations to the PEG, respectively. Assuming a diffusion limited on rate constant for a K^+ ion in water, $k_{on} \approx 10^9 \text{ M}^{-1} \text{ s}^{-1}$, the mean time a cation is bound to the polymer is $\tau = 1 / k_{off} \approx 1$ ns. This is comparable for the mean transit time for a mobile K^+ ion through the pore, which is why even extremely weak binding of cations to PEG can contribute to the polymer-induced decrease in the channel conductance.

3. DNA sequencing with nanopores

The human genome, which is comprised of 3 billion base pairs in 23 chromosomes, encodes for >30,000 proteins. DNA sequence errors *in vivo* can be either beneficial (because the mutations that occur

upon replication promote molecular evolution) or harmful (i.e., cause disease). However, the cost of sequencing a haploid human genome has been prohibitive for routine medical analysis. It is generally understood that the ability to read DNA sequences with high fidelity at significantly lower cost (i.e., less than \$1000/genome) would lead to improved and more accurate diagnosis of disease, better detection of genetic predispositions to cancer, and rational drug design for the population at large.

Reduction of sequencing cost is especially important for the diagnosis and monitoring of specific diseases, including cancer, where the genome can change over time. For instance, genetic markers can be used to monitor the progress of a patient's treatment [113]. This testing involves examining a person's DNA, typically taken from cells in a blood sample, for mutations linked to a disease or disorder. In oncology, doctors use gene testing to diagnose cancer, to classify cancer into subtypes, and to predict a patient's responsiveness to new treatments.

DNA sequencing technology has evolved rapidly since its inception by Gilbert, Sanger, and colleagues [114,115]. Now, a complementary strand of a single strand of the DNA is synthesized enzymatically (by DNA polymerase) in a solution where A, C, G, and T nucleotides with a reaction terminator dideoxynucleotide are sequentially added. The resulting DNA fragments are heat denatured and separated by size using gel electrophoresis. By using four separate reaction vessels each with a different dideoxynucleotide, the relative positions of the different bands are used to read the DNA sequence. Sanger's sequencing by synthesis method was refined in the 1990s and has been implemented into increasingly smaller devices such as miniaturized microtiter plates that permit sequence determination optically from fluorescent tags [116,117] or electrically with CMOS/ISFET technology in massively parallel arrays [118,119].

Other nascent technologies might prove useful for rapid and low-cost sequencing applications. For example, it was shown that individual RNA and DNA polynucleotides could be detected when they are driven electrophoretically through a single protein ion channel [45]. The transport of a single polynucleotide through the pore, in response to an applied electrostatic potential, causes a transient decrease in the ionic current. Moreover, PCR was used to show that single stranded, but not double stranded DNA is completely transported through the alpha-hemolysin pore. On this basis, it was suggested that a nanopore might be able to sequence DNA in a ticker tape fashion if each translocating base caused a distinct current reduction level [45]. That study also mentioned several problems that had to be solved to make the technology feasible. Zoratti and colleagues subsequently used PCR to show that double stranded DNA could transport through the VDAC ion channel [120]. However, the gating properties of VDAC [48] render that pore unsuitable for sequencing applications (Kasianowicz, unpublished observations).

Using single-molecule methods is challenging because molecular properties such as position, speed, force, conformation, and stiffness rely on measuring and interpreting fast transient events on top of significant background noise. Nanopore-based single molecule DNA sequencing relies on the ability to control, in a stepwise motion, a DNA strand (a highly entropic polymer coil) and to read sequence information at each position. However, DNA translocation is fast and subject to Brownian motion. The fundamental issue of why one needs to control the speed at which single stranded DNA molecules migrate through the pore has been discussed elsewhere [29]. Briefly, as noted above, the diffusive motion of a single base past a constriction in the pore would occur too rapidly to identify the base. Thus, DNA-pore interactions need to be tuned in order to slow the polymer's transport rate through the pore. DNA hairpins have been used to locate a single nucleotide pair near the α HL channel's limiting aperture for a sufficient time to allow a distinguishable blockage signature to be recorded. Increasing the solution viscosity, lowering the temperatures (i.e., $<20^\circ\text{C}$), varying molarities and cationic species of the electrolytes solutions cause

modest reductions in translocation velocity of DNA but often come with the adverse effect of reducing the ionic current signal. Thus far, the most successful approaches remain the use of enzymes as a biological motor to control the DNA motion through a nanopore by exploiting interactions between DNA and various processivity enzymes as is described below.

Even with control of the translocation speed, it is critical to understand the mechanism by which DNA bases reduce the current. Unlike synthetic homopolymers, DNA does not simply block the current in a simple relation to the excluded volume of the polynucleotide or bases therein [121]. By fixing DNA to a pore impermeant moiety [37], the length of the pore can be estimated [122], and individual bases can be detected [123]. This method helped create a single sensing region in the α HL pore [124].

Fig. 7 shows two other major approaches considered for DNA sequencing: detecting each base while the single stranded DNA is pulled through the nanopore (right) [125] or by detecting tags that represent the nucleotides during a controlled DNA synthesis by a polymerase [126] (left, i.e. a nanopore-based sequencing by synthesis approach).

Originally, DNA polymerase complexes were used to reduce the rate of DNA translocation through a α HL pore, but not in a controlled manner [127]. Subsequently, Cherf and colleagues used a phi29 DNA polymerase protein attached to a α HL hemolysin, and as the replication proceeds, the DNA strand is ratcheted through the nanopore [128]. The same principle was used by Gundlach and colleagues, where a phi29 DNA polymerase acts as a motor to pull a single strand DNA through a modified MspA pore, resulting in well resolved and reproducible ionic current levels that correspond to individual nucleotide incorporations. The phi29 slows the DNA translocation to ~ 20 to 30 nucleotides per second, which is sufficiently long for base discrimination [129].

Another suggested approach was to attach an *E. coli* exonuclease (ExoI) to a nanopore and read each base as they are cleaved sequentially. Clarke, et al. demonstrated that an α HL channel modified with a covalently linked molecular adapter (β -cyclodextrin) in the pore discriminates well between all four mononucleotides (either added to solution or hydrolyzed by many ExoI enzymes) [130]. However, a theoretical analysis suggested that, in the suggested scheme, the capture probability of the cleaved bases is too small for practical sequencing applications [99]. There are potential technological solutions to the capture problem for such sequencing applications. One such improvement is to use chemical modifiers that modulate the diffusion coefficients of cleaved bases or polymer reporter molecules [131]. Also it is possible to engineer entropic traps to prevent the molecule from diffusing away from the pore [132].

Mammalian DNA is damaged via oxidation at a rate of $\sim 6 \times 10^4$ lesions per cell per day. The damage is typically measured using gas chromatography and mass spectrometry [133]. Recently, White and colleagues used the α HL channel to detect an adduct of a lesion in guanines (8-Oxo-7,8-dihydro-2'-deoxyguanosine) in single-stranded DNA. The method ultimately should prove useful in clinical diagnostic applications and determining the mechanisms by which DNA is damaged and repaired [134,135].

4. MicroRNA detection and identification

MicroRNAs (miRNAs) are a class of nucleic acids containing 18 to 24 nucleotides. The concentration of specific miRNA sequences is correlated with disease, including cancer, making them potentially valuable biomarkers [136–140]. The ability to identify and quantify target miRNA sequences would aid early cancer detection and monitoring disease treatment.

Conventionally, miRNA is detected by hybridizing the target sequence with a labeled, complimentary oligonucleotide probe. The resulting product is analyzed by traditional electrochemical [141] or optical methods, [142,143] and improved throughput can be achieved

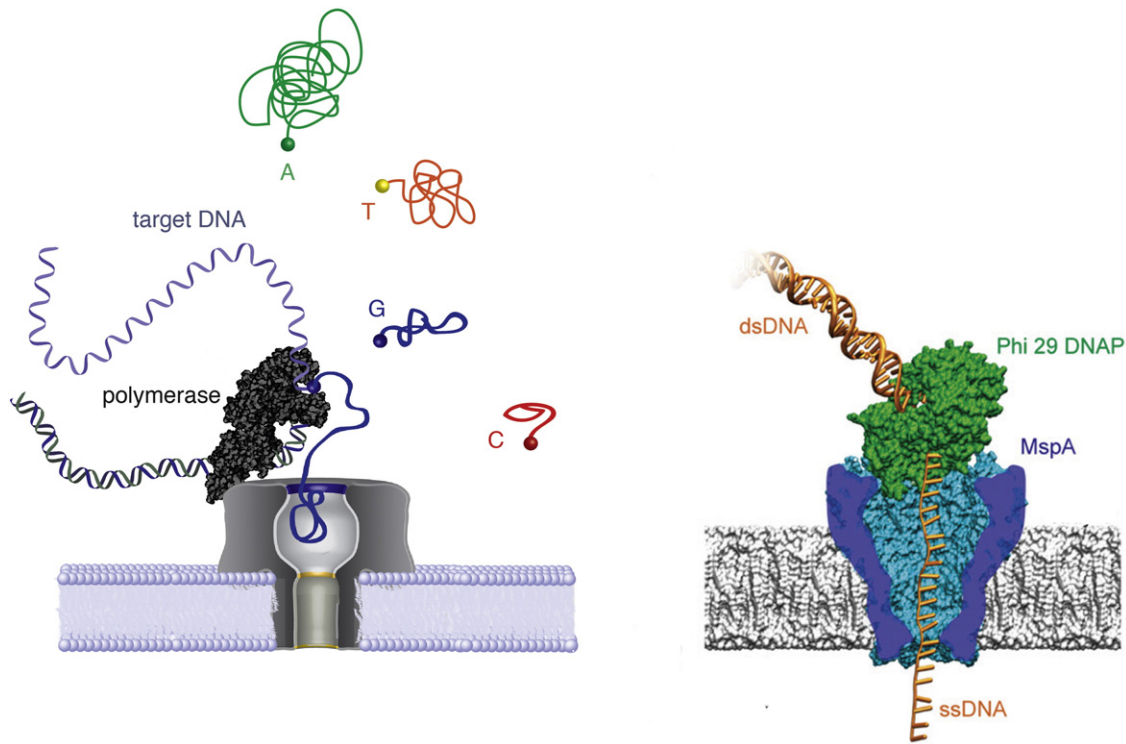


Fig. 7. Two proposed models for sequencing DNA with a single nanopore. (Left) A single molecule sequencing-by-synthesis approach will have the pore read tags, which correspond to each of the 4 DNA bases, after they are cleaved by polymerase attached to the pore [99,126]. (Right) Single stranded DNA is read in a ticker-tape manner [45], and the rate at which bases transport through the pore is controlled by a processivity enzyme [125].

using microarrays [144]. Nanopore-based measurements have been used to detect and characterize relatively long RNA oligonucleotides [45,121]. However, miRNA detection has proven difficult with this system because their residence times are generally too short to unambiguously identify them.

Several methods have been developed to increase the residence time of the miRNA in a nanopore. For example, Wang and colleagues showed that hybridizing a complementary probe RNA molecule to a target miRNA, produced a complex that was easily detected (Fig. 8) [145]. Zhang et al. used a set of barcodes that allow multiple target

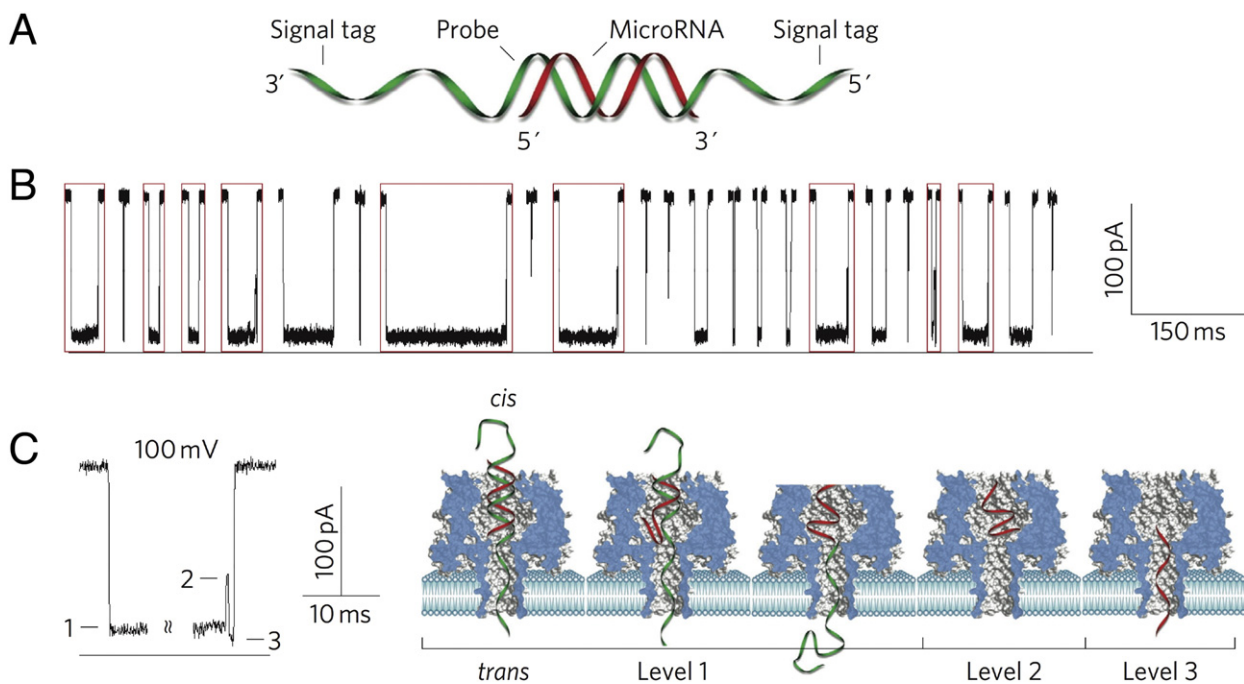


Fig. 8. Detecting and identifying individual microRNAs with the α HL nanopore. (A) Schematic illustration of the target miRNA (red) bound to a longer probe RNA molecule (green) with signal tags on each end. The hybridization of the probe to target miRNA markedly slows down the transport of the latter through the pore. (B) Ionic current time series illustrating the capture of individual complexes by the pore. (C) A typical blockade event caused by a single miRNA:probe RNA complex (left). The three current levels correspond to the different states of the complex (right) [145].

sequences to be identified in a single measurement [146]. Other methods have been developed to increase the residence time of miRNA molecules in a nanopore.

Alternatively, structural or sequence changes to miRNA can allow it to be measured by a nanopore. For example, Zhang and colleagues showed that light-induced small molecule binding to target miRNA produced a detectable signal [147]. While in recent studies, Clamer et al. showed that uridylation of single stranded RNA oligonucleotide can increase its residence in the α HL channel [148].

5. Protein & peptide detection and characterization

While the bulk of nanopore sensing papers focused on nucleic acids, particularly for DNA sequencing, the field is gaining traction for the detection and characterization proteins and small peptides [149]. Proteins and peptides present many experimental variables that do not exist for synthetic polymers or nucleic acids. The complex secondary structure, and distribution of charges along the protein backbone create unique challenges and opportunities for devising nanopore experiments. Although many natively folded proteins are too large to enter the pore, single nanopore sensors were developed to take advantage of known biological interactions, such as the AB-toxins secreted by *B. anthracis* [43]. Movileanu and colleagues mimicked this behavior by modifying the α HL pore with a covalently attached polymer that could bind to a target analyte in solution [150]. Recognition elements can also be engineered into the pore by attaching single peptide recognition elements to the exterior of the pore [151]. In a similar vein, proteins with an electrostatically labeled peptide tag could be captured by α HL engineered to contain electrostatic traps within the β -barrel to capture and hold the analyte [152,153]. By increasing the residence time of the peptides within the nanopore, it is possible to identify hypothetical conformational states of the analyte within the pore [154].

Following the early work on PEG interaction with a n α HL nanopore [44], synthetic peptides were detected with the pore [153,155–157]. The interactions between secondary structural peptides and a nanopore are voltage dependent because of localized charges on the polypeptide chains [156], and polypeptides with opposite terminal charges can be used to control transport within the pore [158]. The repeated unit structure of short polypeptides such as collagen-like peptide helices [159] and (AAKAA)_n-containing polypeptides [155] was provided as a good model to investigate the kinetic rate constants and free energy landscape for proteins inside nanopores. Together, these studies suggest that some degree of secondary structure can be detected as the peptides interact with the pore. Peptide residence times and blockade depths can also be modulated by divalent cations to enable metal ion–peptide interactions [160] and ultimately stereo-selective detection of proteins and peptides [161].

Nanopore-based single molecule detection was not limited merely to intact polymers that could be captured outside the pore [85], or small enough to enter the pore. Oukhaled and colleagues demonstrated that chemical denaturants such as guanidinium-HCl could induce partial unfolding of full-length proteins, which enabled subsequent capture and detection by the native α HL channel [162]. Subsequent work extended the technique to other porins such as aerolysin, which is resistant to chemical denaturation [163,164], and other denaturants such as temperature [102].

Protein folding issues are also related to diseases, including neurodegenerative disorders. Nanopores provide the ability to monitor the real-time dynamic folding of self-aggregated proteins. Wang used the α HL channel to study the structural changes of A β 42 as it interacts with Congo red (self-aggregation inhibitor) and β -cyclodextrin (self-aggregation promoter) [165]. α -Synuclein is another elemental peptide to form fibril of amyloid that is critical to understand the pathogenesis of Parkinson's disease. The monomeric α -synuclein is a natively unfolded peptide with non-uniform surface charge under physiological conditions [166], which is assumed to translocate through

nanopore in a linear fashion. By investigating current blockades under a range of applied voltages different dynamic folding states of α -synuclein monomers were observed [167]. Thus, nanopores provide a new tool to study the dynamic folding states of proteins and polypeptides at the single molecule level.

While the detection of proteins and peptides has been successful with proteinaceous nanopores, the flexibility in size and materials of solid-state nanopores could prove useful here [168–172]. Such pores can be fabricated sufficiently large to observe full-length natively folded proteins, [173–175]. They have also become powerful tools for monitoring folding [173], unfolding and stretching [176,177], and oligomerization of proteins [178]. These methods should become more accessible as high-bandwidth recording becomes *de rigueur* in the nanopore sensing laboratory [179,180].

6. Nanopore-based single molecule force spectroscopy

Nanopores offer a new method for single molecule force spectroscopy studies [181]. They enable many more experiments that can be done in a given time, compared to having target molecules tethered to a solid support. This method follows many of the same principles described above, with the addition of externally applied forces (e.g., electrical, chemical, entropic, or optical tweezer). By modulating any of the latter, the residence time of a polymer in the pore can be altered. Dudko and colleagues revised a theory they developed for AFM or optical tweezer pulling experiments [182,183], which estimates not only intrinsic rate constants, but also localizes the transition state providing a full free-energy surface of a dynamic single molecule pulling experiment [184]. These theories were critically tested by examining the unzipping kinetics of DNA hairpins [181]. Bates and colleagues used the technique to determine the rate at which polynucleotides unzip as a function of the applied potential force-loading rate [185].

A simplified version of this method [85] was used to determine DNA hairpin strength [186]. The free end of the polymer was driven into the α HL channel, but the hairpin remains in the pore's vestibule until the applied electric field eventually disrupts the bonds that hold the hairpin intact. The lifetime of the DNA hairpin correlated with the free energy of hairpin formation and was substantially altered by a single-base mismatch. These methods have proven useful for the determination of base-pair energies as a function of sequence [187], DNA base-pair dynamics [188] and nanopore-DNA geometry [189].

By integrating optical tweezers into a nanopore apparatus, the applied electrostatic force can be balanced with an optical force that act on a DNA molecule-polystyrene bead complex when the DNA is inside the pore [190]. This system was used to control the rate at which individual polymers thread through the pore. In addition, the ability to measure the force on the polymer inside the pore, via an optical tweezer, provides yet another analytical tool to probe inter- and intra-molecular interactions.

Fig. 9 illustrates the use of an enzyme to provide an external force on a protein that is partially inside a nanopore [191,192]. Briefly, an unfoldase enzyme (ClpX from *E. coli*) controls the unfolding and translocation of engineered proteins, and generates sufficient mechanical force to denature a protein (Smt3) by pulling it through the pore. The ionic current traces illustrate the capture of the target Smt3 protein, the ClpX-mediated ramping state, and Smt3 domain unfolding, and eventual translocation of the protein through the nanopore that are illustrated in Fig. 9B. By extending the repeated sequences of engineered Smt3 protein, the blockade states could be tied to sequential unfolding events as the enzyme pulled the protein through the pore (Fig. 9C). To examine whether nanopore devices based on a ClpX-binding tag could be used for protein sequence analysis and identification, three kinds of protein sequences that contain different structure modification and domain variants, which bind to the C-terminal of Smt3 domain, were tested [192]. The translocation rate and blockade states reveal that a nanopore with an enzyme motor could distinguish between individual

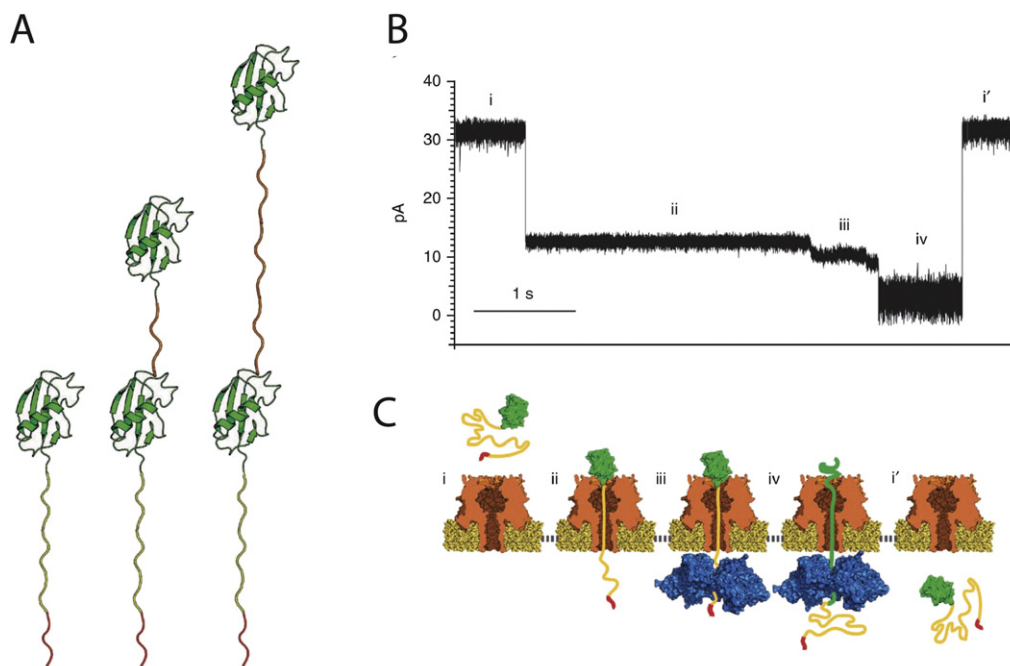


Fig. 9. Nanopore-based single molecule force spectroscopy method for probing protein secondary structure. (A) Schematic illustration of the target protein secondary structure to be studied (green) tethered to a linker with an enzyme recognition site (yellow) and a charged moiety to aid capture by the pore (red). (B) Ionic current times series indicating capture of the charged end of the complex (transition from i to ii), the enzyme attaching to the linker-recognition site (iii), fueled by ATP hydrolysis, the enzyme causes the protein to unfold, thread through the pore (iv) and subsequently exit the pore (i'). (C) Cartoon illustration of the nanopore, and *E. coli* ClpX enzyme (blue) that provides the pulling force on the target protein (green, yellow, and red) [191].

strands between different protein domains in series and variants of these domains in single protein as driven through the α HL nanopore. Qualitatively similar experiments were performed by Rodriguez-Larrea using an engineered thioredoxin protein and the α HL nanopore [193].

7. Temperature-jump spectroscopy for nanopore-based analyses

The majority of single nanopore conductance measurements have focused on resistive-pulse style experiments [29,31]. With such an approach, the kinetic analysis of chemical reactions (e.g., enzyme reactions) or phase transitions in molecules is limited to following the production or consumption of reactants [45,194] or the pore's ability to capture molecules [195–197]. At the single molecule limit, static room temperature equilibrium measurements of molecular interactions place severe limits on the ability to probe reaction kinetics when reaction energy barriers are significantly greater than the thermal energy. The recent demonstration that rapid and controlled temperature changes can be made at the nanopore-bulk solution interface enables a more direct and dynamic route to study single molecule dynamics.

In the 1950s, Eigen and colleagues developed a temperature-jump method to measure “immeasurably fast reactions” [198,199]. Prior to their pioneering work, rapid chemical kinetic measurements were primarily done by mixing reactants rapidly, a process that was limited by the ability to relatively large volumes of liquid [200,201]. Since these T-jump methods were developed, the measurement time scale became shorter with the development of Q-switched lasers [202]. However, the latter technique does not control the time at which the onset of the temperature change occurs.

The ability to extend T-jump spectroscopy to the single molecule level became possible by utilizing the well-known localized surface plasmon resonance effect [203–205]. Visible light is adsorbed by plasmon modes in metallic nanoparticles, and the energy is rapidly transferred to the surrounding region via conduction of the heat to the fluid boundary layer and the diffusion of fluid away from the

particle. The resultant temperature gradient decays inversely proportional to the distance from the particle's surface [206], with characteristic space constant of ~ 5 nm [207]. One or several gold nanoparticles can be used to generate well defined spatial temperature gradients, which can be modulated both in time and magnitude with simple optical components [207].

In this method, metallic nanoparticles were attached directly adjacent to the α HL channel via complimentary DNA strands [207], and subsequently for solid-state nanopores through lithographically-defined gold bow-tie structures [208]. Fig. 10 (upper left) illustrates that as visible light is absorbed by the nanoparticle, heat rapidly transferred into the surrounding solution. Light is focused on the particle-nanopore assembly increasing the current proportionally to the power of incident light (bottom left). Because the heated solution volume is so small (\sim attoliter), the heating and cooling steps display nearly identical kinetics, unlike that of picosecond pulsed lasers which heat a much larger solution volume (picoliters) [207,209], and the pore's conductance was used to estimate the temperature. This new technology was used to study the change in the properties of polymers. It was shown that for a single size PEG polymer, both the ionic current blockade depth and residence time distribution depend on the temperature. The change in residence time was in good agreement with theory (Fig. 10, bottom right) [41,73]. However, the observed shift in the blockade depth is greater than theory predicts, perhaps due to either a shift in the polymer's physical-chemical properties orientation within the channel or a reorganization of the channel itself [58].

In addition to studying reaction kinetics, by scanning the laser beam across the gold-modified pore, the plasmon generated heat can be used as an extremely sensitive measurement of the focal volume of the laser [208]. Computational approaches suggest that plasmon-generated temperature gradients can produce thermophoretic phenomena which can be used to both trap and stretch polymers such as DNA within the confines of the nanopore [210,211].

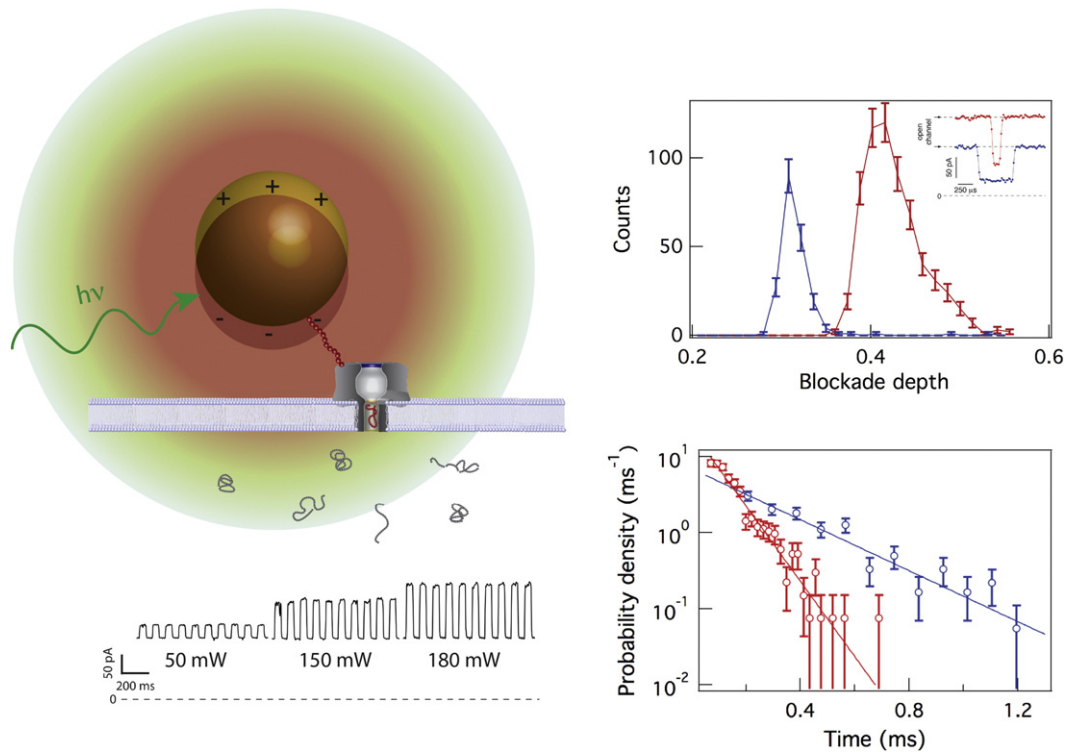


Fig. 10. Single molecule temperature-jump technology. (Top left) Gold nanoparticles attached to the pore are irradiated by visible laser light. The light is absorbed by the particle and converted to heat. The temperature falls off rapidly with distance from the particle. The physical and chemical properties of single molecules near the pore will be altered as the latter diffuse from the bulk to the pore mouth. (Bottom left) A chopped visible light laser beam that is modulated by a Pockels cell alters the pore's current. The degree by which monodisperse length polymers reduce the pore's conductance (top right) and the polymer's residence time distribution depends on the temperature (bottom right) [207].

8. Conclusions

The development of nanopores as single molecule analytical devices has grown considerably in the past two decades. This new metrology was made possible by seminal work by professors Gianfranco Menestrina and Oleg Krasilnikov (who also participated in the field's further development). This review is dedicated to their memory.

Conflict of interest

The authors declare that they have no conflicts of interest with regard to this work.

Acknowledgments

We are grateful for grant support from the NIH NHGRI (R01HG007415), a European Molecular Biology Organization post-doctoral fellowship (to JE), Shenzhen Dedicated Funding of Strategic Emerging Industry Development Program (JCYJ20130408173226864), and the China Postdoctoral Science Foundation (Grant No. 2014M560670).

References

- [1] K.S. Cole, H.J. Curtis, Electric impedance of the squid giant axon during activity, *J. Gen. Physiol.* 22 (1939) 649–670.
- [2] K.S. Cole, Rectification and inductance in the squid giant axon, *J. Gen. Physiol.* 25 (1941) 29–51.
- [3] A.L. Hodgkin, A.F. Huxley, B. Katz, Ionic Currents Underlying Activity in the Giant Axon of the Squid, 3 1949, pp. 129–150.
- [4] A.L. Hodgkin, A.F. Huxley, B. Katz, Measurement of current–voltage relations in the membrane of the giant axon of *Loligo*, *J. Physiol.* 116 (1952) 424–448.
- [5] B. Hille, *Ion Channels of Excitable Membranes*, 3rd ed. Sinauer Associates, Sunderland MA, 2001.
- [6] J.C. Behrends, Evolution of the ion channel concept: the historical perspective, *Chem. Rev.* 112 (2012) 6218–6226.
- [7] A. Parsegian, Energy of an ion crossing a low dielectric membrane: solutions to four relevant electrostatic problems, *Nature* 221 (1969) 844–846.
- [8] G. Ehrenstein, H. Lecar, R. Nossal, The nature of the negative resistance in bimolecular lipid membranes containing excitability-inducing material, *J. Gen. Physiol.* 55 (1970) 119–133.
- [9] C.M. Armstrong, F. Bezanilla, E. Rojas, Destruction of sodium conductance inactivation in squid axons perfused with pronase, *J. Gen. Physiol.* 62 (1973) 375–391.
- [10] C. Miller (Ed.), *Ion Channel Reconstitution*, Springer Science & Business Media, New York, 1986.
- [11] P. Agre, M. Bonhivers, M.J. Borgnia, The aquaporins, blueprints for cellular plumbing systems, *J. Biol. Chem.* 273 (1998) 14659–14662.
- [12] L.S. King, M. Yasui, P. Agre, Aquaporins in health and disease, *Mol. Med. Today* 6 (2000) 60–65.
- [13] L.S. King, D. Kozono, P. Agre, From structure to disease: the evolving tale of aquaporin biology, *Nat. Rev. Mol. Cell Biol.* 5 (2004) 687–698.
- [14] A.L. Harris, Emerging issues of connexin channels: biophysics fills the gap, *Q. Rev. Biophys.* 34 (2001) 325–472.
- [15] B. Katz, *Nerve, Muscle, and Synapse*, McGraw-Hill, New York, 1966.
- [16] F.M. Ashcroft, *Ion Channels and Disease*, Academic Press, San Diego, 1999.
- [17] G. Rouleau, C. Gaspar (Eds.), *Ion Channel Diseases*, 1st ed. Academic Press, San Diego, 2011.
- [18] A.O. Grant, Cardiac ion channels, *Circ. Arrhythm. Electrophysiol.* 2 (2009) 185–194.
- [19] P.M. Quinton, Chloride impermeability in cystic-fibrosis, *Nature* 301 (1983) 421–422.
- [20] D. Doyle, J. Cabral, R. Pfuetzner, A. Kuo, J. Gulbis, S. Cohen, et al., The structure of the potassium channel: molecular basis of K⁺ conduction and selectivity, *Science* 280 (1998) 69–77.
- [21] F.G. van der Goot (Ed.), *Pore-forming Toxins*, Springer Berlin Heidelberg, Berlin, Heidelberg, 2001.
- [22] M.R. Popoff, Bacterial exotoxins, in: W. Russel, H. Herwald (Eds.), *Concepts in Bacterial Virulence*, Karger, Basel 2005, pp. 28–54.
- [23] F.C.O. Los, T.M. Randis, R.V. Aroian, A.J. Ratner, Role of pore-forming toxins in bacterial infectious diseases, *Microbiol. Mol. Biol. Rev.* 77 (2013) 173–207.
- [24] S. Bhakdi, R. Füssle, J. Tranum-Jensen, Staphylococcal alpha-toxin — oligomerization of hydrophilic monomers to form amphiphilic hexamers induced through contact with deoxycholate detergent micelles, *Proc. Natl. Acad. Sci. U. S. A.* 78 (1981) 5475–5479.
- [25] G. Menestrina, Ionic channels formed by *Staphylococcus aureus* alpha-toxin: voltage-dependent inhibition by divalent and trivalent cations, *J. Membr. Biol.* 90 (1986) 177–190.
- [26] M. Niederweis, Mycobacterial porins—new channel proteins in unique outer membranes, *Mol. Microbiol.* 49 (2003) 1167–1177.
- [27] R. Hancock, A. Schmidt, K. Bauer, R. Benz, Role of lysines in ion selectivity of bacterial outer-membrane porins, *Biochim. Biophys. Acta* 860 (1986) 263–267.
- [28] S.B. Hladky, D.A. Haydon, Ion transfer across lipid membranes in the presence of gramicidin A. I. Studies of the unit conductance channel, *Biochim. Biophys. Acta* 274 (1972) 294–312.

- [29] J.J. Kasianowicz, J.W.F. Robertson, E.R. Chan, J.E. Reiner, V.M. Stanford, Nanoscopic porous sensors, *Annu. Rev. Anal. Chem.* 1 (2008) 737–766.
- [30] S. Howorka, Z. Sivy, Nanopore analytics: sensing of single molecules, *Chem. Soc. Rev.* 38 (2009) 2360–2384.
- [31] J.E. Reiner, A. Balijepalli, J.W.F. Robertson, J. Campbell, J. Suehle, J.J. Kasianowicz, Disease detection and management via single nanopore-based sensors, *Chem. Rev.* 112 (2012) 6431–6451.
- [32] J.W.F. Robertson, J.J. Kasianowicz, S. Banerjee, Analytical approaches for studying transporters, channels and porins, *Chem. Rev.* 112 (2012) 6227–6249.
- [33] G. Menestrina, G. Schiavo, C. Montecucco, Molecular mechanisms of action of bacterial protein toxins, *Mol. Asp. Med.* 15 (1994) 79–193.
- [34] J.E. Gouaux, O. Braha, M.R. Hobaugh, L.Z. Song, S. Cheley, C. Shustak, et al., Subunit stoichiometry of staphylococcal alpha-hemolysin in crystals and on membranes – a heptameric transmembrane pore, *Proc. Natl. Acad. Sci. U. S. A.* 91 (1994) 12828–12831.
- [35] L. Song, M. Hobaugh, C. Shustak, S. Cheley, H. Bayley, J.E. Gouaux, Structure of staphylococcal alpha-hemolysin, a heptameric transmembrane pore, *Science* 274 (1996) 1859–1866.
- [36] P.G. Merzlyak, L.N. Yuldasheva, C.G. Rodrigues, C. Carneiro, O.V. Krasilnikov, S.M. Bezrukov, Polymeric nonelectrolytes to probe pore geometry: application to the alpha-toxin transmembrane channel, *Biophys. J.* 77 (1999) 3023–3033.
- [37] S.E. Henrickson, M. Misakian, B. Robertson, J.J. Kasianowicz, Driven DNA transport into an asymmetric nanometer-scale pore, *Phys. Rev. Lett.* 85 (2000) 3057–3060.
- [38] S. Bezrukov, J.J. Kasianowicz, Current noise reveals protonation kinetics and number of ionizable sites in an open protein ion channel, *Phys. Rev. Lett.* 70 (1993) 2352–2355.
- [39] J.J. Kasianowicz, S.M. Bezrukov, Protonation dynamics of the alpha-toxin ion-channel from spectral analysis of pH-dependent current fluctuations, *Biophys. J.* 69 (1995) 94–105.
- [40] J.W.F. Robertson, C.G. Rodrigues, V.M. Stanford, K.A. Rubinson, O.V. Krasilnikov, J.J. Kasianowicz, Single-molecule mass spectrometry in solution using a solitary nanopore, *Proc. Natl. Acad. Sci. U. S. A.* 104 (2007) 8207–8211.
- [41] J.E. Reiner, J.J. Kasianowicz, B.J. Nablo, J.W.F. Robertson, Theory for polymer analysis using nanopore-based single-molecule mass spectrometry, *Proc. Natl. Acad. Sci. U. S. A.* 107 (2010) 12080–12085.
- [42] B. Cornell, V. Braach-Maksyvtis, L. King, P. Osman, B. Raguse, L. Wiczorek, et al., A biosensor that uses ion-channel switches, *Nature* 387 (1997) 580–583.
- [43] K.M. Halverson, R.G. Panchal, T.L. Nguyen, R. Gussio, S.F. Little, M. Misakian, et al., Anthrax biosensor, protective antigen ion channel asymmetric blockade, *J. Biol. Chem.* 280 (2005) 34056–34062.
- [44] S.M. Bezrukov, I. Vodyanoy, R. Brutyanyan, J.J. Kasianowicz, Dynamics and free energy of polymers partitioning into a nanoscale pore, *Macromolecules* 29 (1996) 8517–8522.
- [45] J.J. Kasianowicz, E. Brandin, D. Branton, D.W. Deamer, Characterization of individual polynucleotide molecules using a membrane channel, *Proc. Natl. Acad. Sci. U. S. A.* 93 (1996) 13770–13773.
- [46] O. Braha, B. Walker, S. Cheley, J.J. Kasianowicz, L. Song, J.E. Gouaux, et al., Designed protein pores as components for biosensors, *Chem. Biol.* 4 (1997) 497–505.
- [47] A. Einstein, On the movement of small particles suspended in stationary liquids required by the molecular-kinetic theory of heat, *Ann. Phys.* 17 (1905) 549–560.
- [48] J. Zimmerberg, V.A. Parsegian, Polymer inaccessible volume changes during opening and closing of a voltage-dependent ionic channel, *Nature* 323 (1986) 36–39.
- [49] J. Zimmerberg, F. Bezanilla, V.A. Parsegian, Solute inaccessible aqueous volume changes during opening of the potassium channel of the squid giant-axon, *Biophys. J.* 57 (1990) 1049–1064.
- [50] O.V. Krasilnikov, R.Z. Sabirov, V.I. Ternovsky, P.G. Merzlyak, J.N. Muratkhodjaev, A simple method for the determination of the pore radius of ion channels in planar lipid bilayer-membranes, *FEMS Microbiol. Immunol.* 105 (1992) 93–100.
- [51] G.E. Fanucci, J.Y. Lee, D.S. Cafiso, Spectroscopic evidence that osmolytes used in crystallization buffers inhibit a conformation change in a membrane protein, *Biochemistry* 42 (2003) 13106–13112.
- [52] O.V. Krasilnikov, R.Z. Sabirov, A.N. Chanturla, A.V. Parshikov, The conductivity and latrotoxin channel diameter in lipid bilayer, *60* 1988, pp. 67–71.
- [53] O.V. Krasilnikov, R.Z. Sabirov, V.I. Ternovsky, P.G. Merzlyak, B.A. Tashmukhamedov, The structure of *Staphylococcus aureus* alpha-toxin-induced ionic channel, *Gen. Physiol. Biophys.* 7 (1988) 467–473.
- [54] O.V. Krasilnikov, R.Z. Sabirov, Ion transport through channels formed in lipid bilayers by *Staphylococcus aureus* alpha toxin, *Gen. Physiol. Biophys.* 8 (1989) 213–222.
- [55] O.V. Krasilnikov, C.G. Rodrigues, S.M. Bezrukov, Single polymer molecules in a protein nanopore in the limit of a strong polymer-pore attraction, *Phys. Rev. Lett.* 97 (2006) 018301.
- [56] O.V. Krasilnikov, P.G. Merzlyak, L.N. Yuldasheva, R. Azimova, R. Nogueira, Pore-forming properties of proteolytically nicked staphylococcal alpha-toxin: the ion channel in planar lipid bilayer membranes, *Med. Microbiol. Immunol.* 186 (1997) 53–61.
- [57] O.V. Krasilnikov, S.M. Bezrukov, Polymer partitioning from nonideal solutions into protein voids, *Macromolecules* 37 (2004) 2650–2657.
- [58] J.W.F. Robertson, J.J. Kasianowicz, J.E. Reiner, Changes in ion channel geometry resolved to sub-ångström precision via single molecule mass spectrometry, *J. Phys. Condens. Matter* 22 (2010) 454108.
- [59] R.O. Blaustein, E.J. Lea, A. Finkelstein, Voltage-dependent block of anthrax toxin channels in planar phospholipid bilayer membranes by symmetric tetraalkylammonium ions, *J. Gen. Physiol.* 96 (1990) 905–920.
- [60] R.O. Blaustein, A. Finkelstein, Diffusion limitation in the block by symmetric tetraalkylammonium ions of anthrax toxin channels in planar phospholipid bilayer membranes, *J. Gen. Physiol.* 96 (1990) 943–957.
- [61] B.J. Nablo, K.M. Halverson, J.W.F. Robertson, T.L. Nguyen, R.G. Panchal, R. Gussio, et al., Sizing the *Bacillus anthracis* PA63 channel with nonelectrolyte poly(ethylene glycols), *Biophys. J.* 95 (2008) 1157–1164.
- [62] V.I. Ternovsky, P.A. Grigoriev, G.N. Berestovsky, R. Schlegel, K. Dornberger, U. Gräfe, Effective diameters of ion channels formed by homologs of the antibiotic chrysopermin, *Membr. Cell Biol.* 11 (1997) 497–505.
- [63] C. Goudet, J.-P. Benitah, M.-L. Milat, H. Sentenac, J.-B. Thibaud, Cluster organization and pore structure of ion channels formed by beticolin 3, a nonpeptidic fungal toxin, *Biophys. J.* 77 (1999) 3052–3059.
- [64] O.V. Krasilnikov, J.N. Muratkhodjaev, S.E. Voronov, Y.V. Yezepchuk, The ionic channels formed by cholera toxin in planar bilayer lipid membranes are entirely attributable to its B-subunit, *Biochim. Biophys. Acta* 1067 (1991) 166–170.
- [65] O.S. Ostroumova, P.A. Gurnev, L.V. Schagina, S.M. Bezrukov, Asymmetry of syringomycin E channel studied by polymer partitioning, *FEBS Lett.* 581 (2007) 804–808.
- [66] L.N. Yuldasheva, P.G. Merzlyak, A.O. Zitzer, C.G. Rodrigues, S. Bhakdi, O.V. Krasilnikov, Lumen geometry of ion channels formed by *Vibrio cholerae* EL Tor cytolysin elucidated by nonelectrolyte exclusion, *BBA Biomembr.* 1512 (2001) 53–63.
- [67] O.V. Krasilnikov, V.I. Ternovsky, D.G. Navasardiyants, L.I. Kalmykova, The characterization of ion channels formed by *Pasteurella multocida* dermonecrotic toxin, *Med. Microbiol. Immunol.* 183 (1994) 229–237.
- [68] O.V. Krasilnikov, J. Da Cruz, L. Yuldasheva, W. Varanda, R. Nogueira, A novel approach to study the geometry of the water lumen of ion channels: colicin Ia channels in planar lipid bilayers, *J. Membr. Biol.* 161 (1998) 83–92.
- [69] C.M.M. Carneiro, O.V. Krasilnikov, L.N. Yuldasheva, A.C. Campos de Carvalho, R.A. Nogueira, Is the mammalian porin channel, VDAC, a perfect cylinder in the high conductance State? *Biochem. Biophys. Res. Commun.* 416 (1997) 187–189.
- [70] S. Desai, R. Rosenberg, Pore size of the malaria parasite's nutrient channel, *Proc. Natl. Acad. Sci. U. S. A.* 94 (1997) 2045–2049.
- [71] S. van Dorp, U.F. Keyser, N.H. Dekker, C. Dekker, S.G. Lemay, Origin of the electrophoretic force on DNA in solid-state nanopores, *Nat. Phys.* 5 (2009) 347–351.
- [72] A.G. Lee, Biological membranes: the importance of molecular detail, *Trends Biochem. Sci.* 36 (2011) 493–500.
- [73] A. Balijepalli, J.W.F. Robertson, J.E. Reiner, J.J. Kasianowicz, R.W. Pastor, Theory of polymer-nanopore interactions refined using molecular dynamics simulations, *J. Am. Chem. Soc.* 135 (2013) 7064–7072.
- [74] O.V. Krasilnikov, Sizing channels with neutral polymers, in: J.J. Kasianowicz, M.S. Kellermayer, D.W. Deamer (Eds.), *Structure and Dynamics of Confined Polymers*, Kluwer Academic Publishers, Dordrecht, 2002.
- [75] S.M. Bezrukov, O.V. Krasilnikov, L.N. Yuldasheva, A.M. Berezhkovskii, C.G. Rodrigues, Field-dependent effect of crown ether (18-crown-6) on ionic conductance of α -hemolysin channels, *Biophys. J.* 87 (2004) 3162–3171.
- [76] A.E.P. Schibel, T. Edwards, R. Kawano, W. Lan, H.S. White, Quartz nanopore membranes for suspended bilayer ion channel recordings, *Anal. Chem.* 82 (2010) 7259–7266.
- [77] R.J. White, E.N. Ervin, T. Yang, X. Chen, S. Daniel, P.S. Cremer, et al., Single ion-channel recordings using glass nanopore membranes, *J. Am. Chem. Soc.* 129 (2007) 11766–11775.
- [78] D.K. Shenoy, W.R. Barger, A. Singh, R.G. Panchal, M. Misakian, V.M. Stanford, et al., Functional reconstitution of protein ion channels into planar polymerizable phospholipid membranes, *Nano Lett.* 5 (2005) 1181–1185.
- [79] B.A. Heitz, J. Xu, H.K. Hall, C.A. Aspinwall, S.S. Saavedra, Enhanced long-term stability for single ion channel recordings using suspended poly(lipid) bilayers, *J. Am. Chem. Soc.* 131 (2009) 6662–6663.
- [80] B.A. Heitz, I.W. Jones, H.K. Hall, C.A. Aspinwall, S.S. Saavedra, Fractional polymerization of a suspended planar bilayer creates a fluid, highly stable membrane for ion channel recordings, *J. Am. Chem. Soc.* 132 (2010) 7086–7093.
- [81] T. Thapliyal, J.L. Poulos, J.J. Schmidt, Automated lipid bilayer and ion channel measurement platform, *Biosens. Bioelectron.* 26 (2011) 2651–2654.
- [82] G. Baaken, M. Sondermann, C. Schlemmer, J. Ruehe, J.C. Behrends, Planar microelectrode-cavity array for high-resolution and parallel electrical recording of membrane ionic currents, *Lab Chip* 8 (2008) 938–944.
- [83] G. Baaken, N. Ankr, A.-K. Schuler, J. Rühle, J.C. Behrends, Nanopore-based single-molecule mass spectrometry on a lipid membrane microarray, *ACS Nano* 5 (2011) 8080–8088.
- [84] G. Baaken, I. Halimeh, L. Bacri, J. Pelta, A. Oukhaled, J.C. Behrends, High-resolution size-discrimination of single non-ionic synthetic polymers with a highly charged biological nanopore, *ACS Nano* 9 (2015) 6443–6449.
- [85] J.J. Kasianowicz, S. Henrickson, H. Weetall, B. Robertson, Simultaneous multianalyte detection with a nanometer-scale pore, *Anal. Chem.* 73 (2001) 2268–2272.
- [86] L.-Q. Gu, O. Braha, S. Conlan, S. Cheley, H. Bayley, Stochastic sensing of organic analytes by a pore-forming protein containing a molecular adapter, *Nature* 398 (1999) 686–690.
- [87] L.-Q. Gu, H. Bayley, Interaction of the noncovalent molecular adapter, beta-cyclodextrin, with the staphylococcal alpha-hemolysin pore, *Biophys. J.* 79 (2000) 1967–1975.
- [88] X.-F. Kang, S. Cheley, X. Guan, H. Bayley, Stochastic detection of enantiomers, *J. Am. Chem. Soc.* 128 (2006) 10684–10685.
- [89] E. Campos, C.E. McVey, R.P. Carney, F. Stellacci, Y. Astier, J. Yates, Sensing single mixed-monolayer protected gold nanoparticles by the α -hemolysin nanopore, *Anal. Chem.* 85 (2013) 10149–10158.
- [90] E. Campos, A. Asandei, C.E. McVey, J.C. Dias, A.S.F. Oliveira, C.M. Soares, et al., The role of Lys147 in the interaction between MPSA-gold nanoparticles and the α -hemolysin nanopore, *Langmuir* 28 (2012) 15643–15650.

- [91] C.E. Angevine, A.E. Chavis, N. Kothalawala, A. Dass, J.E. Reiner, Enhanced single molecule mass spectrometry via charged metallic clusters, *Anal. Chem.* 86 (2014) 11077–11085.
- [92] S. Ghosal, Effect of salt concentration on the electrophoretic speed of a polyelectrolyte through a nanopore, *Phys. Rev. Lett.* 98 (2007) 238104.
- [93] S. Ghosal, Electrokinetic-flow-induced viscous drag on a tethered DNA inside a nanopore, *Phys. Rev. E* 76 (2007) 061916.
- [94] D.P. Hoogerheide, F. Albertorio, J.A. Golovchenko, Escape of DNA from a weakly biased thin nanopore: experimental evidence for a universal diffusive behavior, *Phys. Rev. Lett.* 111 (2013) 248301.
- [95] D. Lubensky, D. Nelson, Driven polymer translocation through a narrow pore, *Biophys. J.* 77 (1999) 1824–1838.
- [96] M. Muthukumar, Polymer translocation through a hole, *J. Chem. Phys.* 111 (1999) 10371–10374.
- [97] C. Wei, D. Srivastava, Theory of transport of long polymer molecules through carbon nanotube channels, *Phys. Rev. Lett.* 91 (2003) 235901.
- [98] J.L.A. Dubbeldam, A. Milchev, V.G. Rostiashvili, T.A. Vilgis, Driven polymer translocation through a nanopore: a manifestation of anomalous diffusion, *Europhys. Lett.* 79 (2007) 18002.
- [99] J.E. Reiner, A. Balijepalli, J.W.F. Robertson, B.S. Drown, D.L. Burden, J.J. Kasianowicz, The effects of diffusion on an exonuclease/nanopore-based DNA sequencing engine, *J. Chem. Phys.* 137 (2012) 214903.
- [100] K.I. Lee, S. Jo, H. Rui, B. Egwolf, B. Roux, R.W. Pastor, et al., Web interface for Brownian dynamics simulation of ion transport and its applications to beta-barrel pores, *Am. J. Med. Genet.* 33 (2011) 331–339.
- [101] J. Gidzen, T. Wyttenbach, A.T. Jackson, J.H. Scrivens, M.T. Bowers, Gas-phase conformations of synthetic polymers: poly (ethylene glycol), poly (propylene glycol), and poly (tetramethylene glycol), *J. Am. Chem. Soc.* 122 (2000) 4692–4699.
- [102] L. Payet, M. Martinho, M. Pastoriza-Gallego, J.-M. Betton, L. Auvray, J. Pelta, et al., Thermal unfolding of proteins probed at the single molecule level using nanopores, *Anal. Chem.* 84 (2012) 4071–4076.
- [103] R. DeBlois, C. Bean, Counting and sizing of submicron particles by resistive pulse technique, *Rev. Sci. Instrum.* 41 (1970) 909–916.
- [104] O.A. Saleh, L.L. Sohn, Quantitative sensing of nanoscale colloids using a microchip Coulter counter, *Rev. Sci. Instrum.* 72 (2001) 4449–4451.
- [105] O.A. Saleh, L.L. Sohn, Direct detection of antibody-antigen binding using an on-chip artificial pore, *Proc. Natl. Acad. Sci. U. S. A.* 100 (2003) 820–824.
- [106] T. Ito, L. Sun, R.M. Crooks, Simultaneous determination of the size and surface charge of individual nanopipettes using a carbon nanotube-based Coulter counter, *Anal. Chem.* 75 (2003) 2399–2406.
- [107] T. Ito, L. Sun, R. Henriquez, R.M. Crooks, A carbon nanotube-based Coulter nanoparticle counter, *Acc. Chem. Res.* 37 (2004) 937–945.
- [108] A. Carbonaro, L.L. Sohn, A resistive-pulse sensor chip for multianalyte immunoassays, *Lab Chip* 5 (2005) 1155–1160.
- [109] P.-G. de Gennes, *Scaling Concepts in Polymer Physics*, Cornell University Press, Ithaca and London, 1979.
- [110] K. Stojilkovic, A.M. Berezkhovskii, V. Zitserman, S.M. Bezrukov, Conductivity and microviscosity of electrolyte solutions containing polyethylene glycols, *J. Chem. Phys.* 119 (2003) 6973–6978.
- [111] M. Mooney, On an indeterminate integral in Einstein's theory of the viscosity of a suspension, *J. Appl. Phys.* 25 (1954) 406–407.
- [112] M.-F. Breton, F. Discala, L. Bacri, D. Foster, J. Pelta, A. Oulchald, Exploration of neutral versus polyelectrolyte behavior of poly(ethylene glycol)s in alkali ion solutions using single-nanopore recording, *J. Phys. Chem. Lett.* 4 (2013) 2202–2208.
- [113] Y. He, J. Wu, D.C. Dressman, C. Lacobuzio-Donahue, S.D. Markowitz, V.E. Velculescu, et al., Heteroplasmic mitochondrial DNA mutations in normal and tumour cells, *Nature* 464 (2010) 610–614.
- [114] F. Sanger, S. Nicklen, A.R. Coulson, DNA sequencing with chain-terminating inhibitors, *Proc. Natl. Acad. Sci. U. S. A.* 74 (1977) 5463–5467.
- [115] A.M. Maxam, W. Gilbert, A new method for sequencing DNA, *Proc. Natl. Acad. Sci. U. S. A.* 74 (1977) 560–564.
- [116] M. Castoldi, A sensitive array for microRNA expression profiling (miChip) based on locked nucleic acids (LNA), *RNA* 12 (2006) 913–920.
- [117] D.A. Wheeler, M. Srinivasan, M. Egholm, Y. Shen, L. Chen, A. McGuire, et al., The complete genome of an individual by massively parallel DNA sequencing, *Nature* 452 (2008) 872–876.
- [118] J.M. Rothberg, W. Hinze, T.M. Rearick, J. Schultz, W. Mileski, M. Davey, et al., An integrated semiconductor device enabling non-optical genome sequencing, *Nature* 475 (2011) 348–352.
- [119] B. Merriman, I.T. R D Team, J.M. Rothberg, Progress in Ion Torrent semiconductor chip based sequencing, *Electrophoresis* 33 (2012) 3397–3417.
- [120] I. Szabo, G. Bathori, F. Tombola, M. Brini, A. Coppola, M. Zoratti, DNA translocation across planar bilayers containing *Bacillus subtilis* ion channels, *J. Biol. Chem.* 272 (1997) 25275–25282.
- [121] M. Akeson, D. Branton, J.J. Kasianowicz, E. Brandin, D.W. Deamer, Microsecond time-scale discrimination among polycytidylic acid, polyadenylic acid, and polyuridylic acid as homopolymers or as segments within single RNA molecules, *Biophys. J.* 77 (1999) 3227–3233.
- [122] S.E. Henrickson, E.A. DiMarzio, Q. Wang, V.M. Stanford, J.J. Kasianowicz, Probing single nanometer-scale pores with polymeric molecular rulers, *J. Chem. Phys.* 132 (2010) 135101.
- [123] R.F. Purnell, J.J. Schmidt, Discrimination of single base substitutions in a DNA strand immobilized in a biological nanopore, *ACS Nano* 3 (2009) 2533–2538.
- [124] E.N. Ervin, G.A. Barrall, P. Pal, M.K. Bean, A.E.P. Schibel, A.D. Hibbs, Creating a single sensing zone within an alpha-hemolysin pore via site directed mutagenesis, *Bionanoscience* 4 (2014) 78–84.
- [125] A.H. Laszlo, I.M. Derrington, H. Brinkerhoff, K.W. Langford, I.C. Nova, J.M. Samson, et al., Detection and mapping of 5-methylcytosine and 5-hydroxymethylcytosine with nanopore MspA, *Proc. Natl. Acad. Sci. U. S. A.* 110 (2013) 18904–18909.
- [126] S. Kumar, C. Tao, M. Chien, B. Hellner, A. Balijepalli, J.W.F. Robertson, et al., PEG-labeled nucleotides and nanopore detection for single molecule DNA sequencing by synthesis, *Sci. Rep.* 2 (2012) 684.
- [127] S. Benner, R.J.A. Chen, N.A. Wilson, R. Abu-Shumays, N. Hurt, K.R. Lieberman, et al., Sequence-specific detection of individual DNA polymerase complexes in real time using a nanopore, *Nat. Nanotechnol.* 2 (2007) 718–724.
- [128] G.M. Cherf, K.R. Lieberman, H. Rashid, C.E. Lam, K. Karplus, M. Akeson, Automated forward and reverse ratcheting of DNA in a nanopore at 5-Å precision, *Nat. Biotechnol.* 30 (2012) 344–348.
- [129] E.A. Manrao, I.M. Derrington, A.H. Laszlo, K.W. Langford, M.K. Hopper, N. Gillgren, et al., Reading DNA at single-nucleotide resolution with a mutant MspA nanopore and phi29 DNA polymerase, *Nat. Biotechnol.* 30 (2012) 349–353.
- [130] J. Clarke, H.-C. Wu, L. Jayasinghe, A. Patel, S. Reid, H. Bayley, Continuous base identification for single-molecule nanopore DNA sequencing, *Nat. Nanotechnol.* 4 (2009) 265–270.
- [131] K.T. Brady, J.E. Reiner, Improving the prospects of cleavage-based nanopore sequencing engines, *J. Chem. Phys.* 143 (2015) 074904.
- [132] X. Liu, M. Mihovilovic Skanata, D. Stein, Entropic cages for trapping DNA near a nanopore, *Nat. Commun.* 6 (2015) 6222.
- [133] P. Jaruga, M. Birincioğlu, H. Rodriguez, M. Dizdaroglu, Mass spectrometric assays for the tandem lesion 8,5'-cyclo-2'-deoxyguanosine in mammalian DNA, *Biochemistry* 41 (2002) 3703–3711.
- [134] A.E.P. Schibel, N. An, Q. Jin, A.M. Fleming, C.J. Burrows, H.S. White, Nanopore detection of 8-oxo-7,8-dihydro-2'-deoxyguanosine in immobilized single-stranded DNA via adduct formation to the DNA damage site, *J. Am. Chem. Soc.* 132 (2010) 17992–17995.
- [135] Q. Jin, A.M. Fleming, C.J. Burrows, H.S. White, Unzipping kinetics of duplex DNA containing oxidized lesions in an α -hemolysin nanopore, *J. Am. Chem. Soc.* 134 (2012) 11006–11011.
- [136] M.V. Iorio, M. Ferracin, C.-G. Liu, A. Veronese, R. Spizzo, S. Sabbioni, et al., MicroRNA gene expression deregulation in human breast cancer, *Cancer Res.* 65 (2005) 7065–7070.
- [137] S. Volinia, G.A. Calin, C.-G. Liu, S. Ambs, A. Cimmino, F. Petrocca, et al., A microRNA expression signature of human solid tumors defines cancer gene targets, *Proc. Natl. Acad. Sci. U. S. A.* 103 (2006) 2257–2261.
- [138] M.V. Iorio, R. Visone, G. Di Leva, V. Donati, F. Petrocca, P. Casalini, et al., MicroRNA signatures in human ovarian cancer, *Cancer Res.* 67 (2007) 8699–8707.
- [139] C.L. Bartels, G.J. Tsongalis, MicroRNAs: novel biomarkers for human cancer, *Clin. Chem.* 55 (2009) 623–631.
- [140] F. Petrocca, D. Iliopoulos, H.R. Qin, M.S. Nicoloso, S. Yendamuri, S.E. Wojcik, et al., Alterations of the tumor suppressor gene ARLTS1 in ovarian cancer, *Cancer Res.* 66 (2006) 10287–10291.
- [141] M. Bartosik, R. Hrstka, E. Palecek, B. Vojtesek, *Anal. Chim. Acta* 813 (2014) 35–40.
- [142] L.A. Neely, S. Patel, J. Garver, M. Gallo, M. Hackett, S. McLaughlin, et al., A single-molecule method for the quantitation of microRNA gene expression, *Nat. Methods* 3 (2006) 41–46.
- [143] K.-H. Yeom, I. Heo, J. Lee, S. Hohng, V.N. Kim, C. Joo, *Sci. Rep.* 12 (2011) 690–696.
- [144] H. Dong, J. Lei, L. Ding, Y. Wen, H. Ju, X. Zhang, MicroRNA: Function, Detection, and Bioanalysis, 113 2013, pp. 6207–6233.
- [145] Y. Wang, D. Zheng, Q. Tan, M.X. Wang, L.-Q. Gu, Nanopore-based detection of circulating microRNAs in lung cancer patients, *Nat. Nanotechnol.* 6 (2011) 668–674.
- [146] X. Zhang, Y. Wang, B.L. Fricke, L.-Q. Gu, Programming nanopore ion flow for encoded multiplex microRNA detection, *ACS Nano* 8 (2014) 3444–3450.
- [147] X. Zhang, J. Zhang, Y.-L. Ying, H. Tian, Y.-T. Long, Single molecule analysis of light-regulated RNA:spiropyran interactions, *Chem. Sci.* 5 (2014) 2642.
- [148] M. Clamer, L. Höfler, E. Mikhailova, G. Viero, H. Bayley, Detection of 3'-end RNA uridylation with a protein nanopore, *ACS Nano* 8 (2014) 1364–1374.
- [149] L. Movileanu, Interrogating single proteins through nanopores: challenges and opportunities, *Trends Biotechnol.* 27 (2009) 333–341.
- [150] L. Movileanu, S. Howorka, O. Braha, H. Bayley, Detecting protein analytes that modulate transmembrane movement of a polymer chain within a single protein pore, *Nat. Biotechnol.* 18 (2000) 1091–1095.
- [151] L. Harrington, S. Cheley, L.T. Alexander, S. Knapp, H. Bayley, Stochastic detection of Pim protein kinases reveals electrostatically enhanced association of a peptide substrate, *Proc. Natl. Acad. Sci. U. S. A.* 110 (2013) E4417–E4426.
- [152] M.M. Mohammad, S. Prakash, A. Matouschek, L. Movileanu, Controlling a single protein in a nanopore through electrostatic traps, *J. Am. Chem. Soc.* 130 (2008) 4081–4088.
- [153] A.J. Wolfe, M.M. Mohammad, S. Cheley, H. Bayley, L. Movileanu, Catalyzing the translocation of polypeptides through attractive interactions, *J. Am. Chem. Soc.* 129 (2007) 14034–14041.
- [154] L. Mereuta, M. Roy, A. Asandei, J.-K. Lee, Y. Park, I. Andricioaei, et al., Slowing down single-molecule trafficking through a protein nanopore reveals intermediates for peptide translocation, *Sci. Rep.* 4 (2014) 10419.
- [155] L. Movileanu, J.P. Schmittschmitt, J. Martin Scholtz, H. Bayley, Interactions of peptides with a protein pore, *Biophys. J.* 89 (2005) 1030–1045.
- [156] R. Stefureac, Y.-T. Long, H.-B. Kraatz, P. Howard, J.S. Lee, Transport of alpha-helical peptides through alpha-hemolysin and aerolysin pores, *Biochemistry* 45 (2006) 9172–9179.
- [157] C.P. Goodrich, S. Kirmizialtin, B.M. Huyghues-Despointes, A. Zhu, J.M. Scholtz, D.E. Makarov, et al., Single-molecule electrophoresis of beta-hairpin peptides by

- electrical recordings and Langevin dynamics simulations, *J. Phys. Chem. B* 111 (2007) 3332–3335.
- [158] A. Asandei, M. Chinappi, J.-K. Lee, C. Ho Seo, L. Mereuta, Y. Park, et al., Placement of oppositely charged aminoacids at a polypeptide termini determines the voltage-controlled braking of polymer transport through nanometer-scale pores, *Sci. Rep.* 5 (2015) 10419.
- [159] T.C. Sutherland, Y.T. Long, R.I. Stefureac, I. Bediako-Amoa, H.B. Kraatz, J.S. Lee, Structure of peptides investigated by nanopore analysis, *Nano Lett.* 4 (2004) 1273–1277.
- [160] L. Mereuta, I. Schiopu, A. Asandei, Y. Park, K.-S. Hahn, T. Luchian, Protein nanopore-based, single-molecule exploration of copper binding to an antimicrobial-derived, histidine-containing chimera peptide, *Langmuir* 28 (2012) 17079–17091.
- [161] I. Schiopu, S. Iftemi, T. Luchian, Nanopore Investigation of the Stereoselective Interactions between Cu^{2+} and D,L-Histidine Amino Acids Engineered into an Amyloidic Fragment Analogue, *Langmuir* 31 (2015) 387–396.
- [162] G. Oukhaled, J. Mathe, A.-L. Biance, L. Bacri, J.-M. Betton, D. Lairez, et al., Unfolding of proteins and long transient conformations detected by single nanopore recording, *Phys. Rev. Lett.* 98 (2007) 158101.
- [163] M. Pastoriza-Gallego, L. Rabah, G. Gibrat, B. Thiebot, F.G. van der Goot, L. Auvray, et al., Dynamics of unfolded protein transport through an aerolysin pore, *J. Am. Chem. Soc.* 133 (2011) 2923–2931.
- [164] C. Merstorf, B. Cressiot, M. Pastoriza-Gallego, A. Oukhaled, J.-M. Betton, L. Auvray, et al., Wild type, mutant protein unfolding and phase transition detected by single-nanopore recording, *ACS Chem. Biol.* 7 (2012) 652–658.
- [165] H.-Y. Wang, Y.-L. Ying, Y. Li, H.-B. Kraatz, Y.-T. Long, Nanopore analysis of beta-amyloid peptide aggregation transition induced by small molecules, *Anal. Chem.* 83 (2011) 1746–1752.
- [166] W.G. Hoyer, D. Cherny, V. Subramaniam, T.M. Jovin, Rapid self-assembly of alpha-synuclein observed by in situ atomic force microscopy, *J. Mol. Biol.* 340 (2004) 127–139.
- [167] H.-Y. Wang, Z. Gu, C. Cao, J. Wang, Y.-T. Long, Analysis of a single α -synuclein fibrillation by the interaction with a protein nanopore, *Anal. Chem.* 85 (2013) 8254–8261.
- [168] J. Li, D. Stein, C. McMullan, D. Branton, M. Aziz, J.A. Golovchenko, Ion-beam sculpting at nanometre length scales, *Nature* 412 (2001) 166–169.
- [169] M.J. Kim, M. Wanunu, D.C. Bell, A. Meller, Rapid fabrication of uniformly sized nanopores and nanopore arrays for parallel DNA analysis, *Adv. Mater.* 18 (2006) 3149–3153.
- [170] H.B. George, D.P. Hoogerheide, C.S. Madi, D.C. Bell, J.A. Golovchenko, M.J. Aziz, Ion-sculpting of nanopores in amorphous metals, semiconductors, and insulators, *Appl. Phys. Lett.* 96 (2010) 263111.
- [171] K. Briggs, H. Kwok, V. Tabard-Cossa, Automated fabrication of 2-nm solid-state nanopores for nucleic acid analysis, *Small* 10 (2014) 2077–2086.
- [172] J. Larkin, R. Henley, D.C. Bell, T. Cohen-Karni, J.K. Rosenstein, M. Wanunu, Slow DNA transport through nanopores in hafnium oxide membranes, *ACS Nano* 7 (2013) 10121–10128.
- [173] D.S. Talaga, J. Li, Single-molecule protein unfolding in solid state nanopores, *J. Am. Chem. Soc.* 131 (2009) 9287–9297.
- [174] D. Fologea, B. Ledden, D.S. McNabb, J. Li, Electrical characterization of protein molecules by a solid-state nanopore, *Appl. Phys. Lett.* 91 (2007) 053901.
- [175] E.C. Yusko, J.M. Johnson, S. Majd, P. Prangko, R.C. Rollings, J. Li, et al., Controlling protein translocation through nanopores with bio-inspired fluid walls, *Nat. Nanotechnol.* 6 (2011) 253–260.
- [176] K.J. Freedman, M. Jurgens, A. Prabhu, C.W. Ahn, P. Jemth, J.B. Edel, et al., Chemical, thermal, and electric field induced unfolding of single protein molecules studied using nanopores, *Anal. Chem.* 83 (2011) 5137–5144.
- [177] K.J. Freedman, S.R. Haq, J.B. Edel, P. Jemth, M.J. Kim, Single molecule unfolding and stretching of protein domains inside a solid-state nanopore by electric field, *Sci. Rep.* 3 (2013) 1638.
- [178] D.J. Niedzwiecki, C.J. Lanci, G. Shemer, P.S. Cheng, J.G. Saven, M. Drndic, Observing Changes in the Structure and Oligomerization State of a Helical Protein Dimer Using Solid-State Nanopores, *ACS Nano* (2015) <http://dx.doi.org/10.1021/acsnano.5b02714>.
- [179] J.K. Rosenstein, M. Wanunu, C.A. Merchant, M. Drndic, K.L. Shepard, Integrated nanopore sensing platform with sub-microsecond temporal resolution, *Nat. Methods* 9 (2012) 487–494.
- [180] J. Larkin, R.Y. Henley, M. Muthukumar, J.K. Rosenstein, M. Wanunu, High-bandwidth protein analysis using solid-state nanopores, *Biophys. J.* 106 (2014) 696–704.
- [181] O.K. Dudko, J. Mathe, A. Szabo, A. Meller, G. Hummer, Extracting kinetics from single-molecule force spectroscopy: nanopore unzipping of DNA hairpins, *Biophys. J.* 92 (2007) 4188–4195.
- [182] O. Dudko, A. Filippov, J. Klafter, M. Urbakh, Dynamic force spectroscopy: a Fokker-Planck approach, *Chem. Phys. Lett.* 352 (2002) 499–504.
- [183] O. Dudko, A. Filippov, J. Klafter, M. Urbakh, Beyond the conventional description of dynamic force spectroscopy of adhesion bonds, *Proc. Natl. Acad. Sci. U. S. A.* 100 (2003) 11378–11381.
- [184] O. Dudko, G. Hummer, A. Szabo, Intrinsic rates and activation free energies from single-molecule pulling experiments, *Phys. Rev. Lett.* 96 (2006) 108101.
- [185] M. Bates, M. Burns, A. Meller, Dynamics of DNA molecules in a membrane channel probed by active control techniques, *Biophys. J.* 84 (2003) 2366–2372.
- [186] W. Vercoutere, S. Winters-Hilt, H. Olsen, D. Deamer, D. Haussler, M. Akeson, Rapid discrimination among individual DNA hairpin molecules at single-nucleotide resolution using an ion channel, *Nat. Biotechnol.* 19 (2001) 248–252.
- [187] V. Viasnoff, N. Chiaruttini, U. Bockelmann, Probing DNA base pairing energy profiles using a nanopore, *Eur. Biophys. J. Biophys. Lett.* 38 (2009) 263–269.
- [188] V. Viasnoff, N. Chiaruttini, J. Muzard, U. Bockelmann, Force fluctuations assist nanopore unzipping of DNA, *J. Phys. Condens. Matter* 22 (2010) 454122.
- [189] J. Muzard, M. Martinho, J. Mathe, U. Bockelmann, V. Viasnoff, DNA translocation and unzipping through a nanopore: some geometrical effects, *Biophys. J.* 98 (2010) 2170–2178.
- [190] U.F. Keyser, B.N. Koeleman, S. van Dorp, D. Krapf, R.M.M. Smeets, S.G. Lemay, et al., Direct force measurements on DNA in a solid-state nanopore, *Nat. Phys.* 2 (2006) 473–477.
- [191] J. Nivala, D.B. Marks, M. Akeson, Unfoldase-mediated protein translocation through an α -hemolysin nanopore, *Nat. Biotechnol.* 31 (2013) 247–250.
- [192] J. Nivala, L. Mulrone, G. Li, J. Schreiber, M. Akeson, Discrimination among protein variants using an unfoldase-coupled nanopore, *ACS Nano* 8 (2014) 12365–12375.
- [193] D. Rodriguez-Larrea, H. Bayley, Multistep protein unfolding during nanopore translocation, *Nat. Nanotechnol.* 8 (2013) 288–295.
- [194] M. Kukwikila, S. Howorka, Electrically sensing protease activity with nanopores, *J. Phys. Condens. Matter* 22 (2010) 454103.
- [195] S. Howorka, L. Moviceanu, X. Lu, M. Magnon, S. Cheley, O. Braha, et al., A protein pore with a single polymer chain tethered within the lumen, *J. Am. Chem. Soc.* 122 (2000) 2411–2416.
- [196] L. Moviceanu, S. Cheley, S. Howorka, O. Braha, H. Bayley, Location of a constriction in the lumen of a transmembrane pore by targeted covalent attachment of polymer molecules, *J. Gen. Physiol.* 117 (2001) 239–251.
- [197] L. Moviceanu, H. Bayley, Partitioning of a polymer into a nanoscopic protein pore obeys a simple scaling law, *Proc. Natl. Acad. Sci. U. S. A.* 98 (2001) 10137–10141.
- [198] G. Czerlinski, M. Eigen, Eine temperatursprungmethode Zur untersuchung chemischer relaxation, *Z. Elektrochem.* 63 (1959) 652–661.
- [199] M. Eigen, G. Hammes, Kinetic studies of ADP reactions with the temperature jump method, *J. Am. Chem. Soc.* 82 (1960) 5951–5952.
- [200] B. Chance, The accelerated flow method for rapid reactions. Part I. Analysis, *J. Frankl. Inst.* 229 (1940) 613–640.
- [201] B. Chance, The accelerated flow method for rapid reactions. Part II. Design, construction, and tests, *J. Frankl. Inst.* 229 (1940) 737–766.
- [202] H. Hoffmann, E. Yeager, J. Steuhr, Laser temperature-jump apparatus for relaxation studies in electrolytic solutions, *Rev. Sci. Instrum.* 39 (1968) 649–653.
- [203] W. Knoll, Interfaces and thin films as seen by bound electromagnetic waves, *Annu. Rev. Phys. Chem.* 49 (1998) 569–638.
- [204] E.A. Coronado, E.R. Encina, F.D. Stefani, Optical properties of metallic nanoparticles: manipulating light, heat and forces at the nanoscale, *Nanoscale* 3 (2011) 4042.
- [205] K.A. Willets, R.P. Van Duyne, Localized surface plasmon resonance spectroscopy and sensing, *Annu. Rev. Phys. Chem.* 58 (2007) 267–297.
- [206] Y. Seol, A.E. Carpenter, T.T. Perkins, Gold nanoparticles: enhanced optical trapping and sensitivity coupled with significant heating, *Opt. Lett.* 31 (2006) 2429–2431.
- [207] J.E. Reiner, J.W.F. Robertson, D.L. Burden, L.K. Burden, A. Balijepalli, J.J. Kasianowicz, Temperature sculpting in yoctoliter volumes, *J. Am. Chem. Soc.* 135 (2013) 3087–3094.
- [208] M.P. Jonsson, C. Dekker, Plasmonic nanopore for electrical profiling of optical intensity landscapes, *Nano Lett.* 13 (2013) 1029–1033.
- [209] E.D. Holmstrom, D.J. Nesbitt, Real-time infrared overtone laser control of temperature in picoliter H_2O samples: “nanobathubs” for single molecule microscopy, *J. Phys. Chem. Lett.* 1 (2010) 2264–2268.
- [210] M. Belkin, C. Maffeo, D.B. Wells, A. Aksimentiev, Stretching and controlled motion of single-stranded DNA in locally heated solid-state nanopores, *ACS Nano* 7 (2013) 6816–6824.
- [211] M. Belkin, S.-H. Chao, G. Giannetti, A. Aksimentiev, Modeling thermophoretic effects in solid-state nanopores, *J. Comput. Electron.* 13 (2014) 826–838.
- [212] M. Faller, M. Niederweis, G. Schulz, The structure of a mycobacterial outer-membrane channel, *Science* 303 (2004) 1189–1192.
- [213] S.W. Cowan, T. Schirmer, G. Rummel, M. Steiert, R. Ghosh, R.A. Pauptit, et al., Crystal structures explain functional properties of two *E. coli* porins, *Nature* 358 (1992) 727–733.
- [214] A.L. Lomize, V.Y. Orekhov, A.S. Arsen'ev, Refinement of the spatial structure of the gramicidin ion channel, *Bioorg. Khim.* 18 (1992) 182–200.
- [215] S.M. Bezrukov, J.J. Kasianowicz, The charge state of an ion channel controls neutral polymer entry into its pore, *Eur. Biophys. J.* 26 (1997) 471–476.